Publications

Available Online

JOURNAL OF
SCIENTIFIC RESEARCH

J. Sci. Res. **18** (3), 511-545 (2026)

www.banglajol.info/index.php/JSR

Bayesian and Classical Approaches for Reliability Modeling of Microcircuit Failure Times Using a Lambda Power Exponential Type Distribution

L. B. Sah Telee*

Department of Management Science, Nepal Commerce Campus, Tribhuvan University, Kathmandu, Nepal

Received 10 March 2026, accepted in final revised form 24 June 2026

Abstract

This study introduces a new three-parameter lifetime distribution, the Lambda Power Exponential Type (LPET) distribution derived via Lehmann type-I exponentiation of an exponential Extension baseline using power transformation. A frailty-like shape parameter (α) and a power-based transformation is introduced. The addition of a shape parameter enhances the model flexibility to capture diverse hazard shapes such as decreasing, increasing, bathtub, j-shaped and inverted j- shaped. Both classical maximum likelihood estimation (MLE) and Bayesian analysis using Hamiltonian Monte Carlo (HMC) are employed for the parameter estimation. A Monte Carlo simulation demonstrates a very consistent reduction of both biases, mean square error, and root mean squared error with increasing sample size. Application to real-world microcircuit electromigration failure data verifies the superiority of the LPET model compared to eleven competing lifetime models based on information criteria and goodness of fit tests. Bayesian inference confirms stability of the parameter estimates and aligns closely with Kaplan-Meier survival curve, with a mean time to failure of 7.15 hours and median time to failure of 7.08 hours. The LPET model emerges as a highly flexible and robust model for reliability engineering, survival analysis and time - to-event modeling.

Keywords: Bayesian Inference; Kaplan-Meier Survival; MCMC convergence; Novel Probability distribution; Time to failure study.

doi: https://dx.doi.org/10.3329/jsr.v18i3.88266 J. Sci. Res. **18** (3), 511-545 (2026)

1. Introduction

Reliability analysis also known as time to failure analysis is one of the most important fields in engineering and industrial context. Accurate modeling of time-to-event modeling, we need complex patterns across different time-course stage. In reliability and survival study, mean and median reliability time are the primary interest. An effective lifetime must contain some fundamental failure regimes: early failures caused by decreasing failure rates, random failures that are the results of constant failure rate usually happen during useful life, and wear-out failures characterized by increasing failure rates that indicates the material degradation. Modern reliability datasets- especially under electronic and microcircuit

* *Corresponding author*: lalbabu3131@gmail.com

systems frequently exhibit composite or non-monotonic hazard rate patterns such as decreasing, increasing, bathtub, j-shaped and inverted j-shaped. Many classical models such as exponential, Weibull, Lognormal and Gamma fail to capture these complex behaviors adequately.

Traditional probability models including Exponential, Weibull, gamma, and Lognormal have been widely used but often fail to describe complex data and provide flexibility in hazard rate function [1]. Their limitations in capturing multi-phase hazard behaviors are highlighted in comparative studies [2,3]. Microcircuits frequently behave with non-monotonic hazard rates. Modern real data sets with bathtub, *j*-shaped or inverted bathtub real data sets often need more flexible robust probability models. Also, Classical models may misfit tails or shoulder hazards, recent generalized probability models are capable of capturing skewed as well as bathtub-type hazard rate curves. Despite various advances in exponentiated and power-transformed families, integration of Lehmann exponentiations along with a power transformation on x to jointly control shape as well as failure accumulation are not studied. Existing models generally fail to simultaneously capture all five hazard shapes, especially for microcircuit electromigration datasets with multi-phase hazard rate behaviors.

Exponentiated families-such as the Exponentiated Weibull (EW) [3], Exponentiated Generalized Gamma [4] and Exponentiated Exponential [5] have excellent shape flexibility but still cannot generate all hazard patterns, especially combined bathtub-*j*-shaped transitions. Furthermore, standard exponentiation does not modify the growth rate of input variable and fails to control tails. These limitations have led to generalization of lifetime models to obtain more flexible models. Although many transformation techniques are available, exponentiation and scaling are powerful tools for achieving more accurate and flexible models [6]. Recent work [7] demonstrated generating more flexible novel probability distributions using fractional derivative approaches, further expanding the toolkit for lifetime modeling. The novelty & contribution of the Lambda Power Exponential Type (LPET) model is the unique combination of Lehmann exponentiation and power transformation, resulting in more flexible hazard rate shapes while maintaining parameter interpretability. Lehmann-type exponentiation is used because it is a proven and more powerful method of generating more flexible probability models from baseline distribution. Introduction of a new shape parameter (α) directly controls skewness, kurtosis and tail weight, capturing non monotonic hazard shapes in reliability studies. The parameter α also acts as a frailty parameter controlling unobserved heterogeneity in a population [8].

While exponentiated-G families are well-known, their properties depend heavily on the baseline distribution. The exponentiation of an Exponential Extension baseline generates a unique combination of hazard shapes and tail behaviors not achievable by other popular exponentiated families. The LPET model capture variations in tail behaviors and hazard rates, making it very useful in reliability engineering, risk management, survival analysis and modeling of new probability distributions. Both classical maximum likelihood estimation (MLE) and Bayesian approach were applied to study the robustness of the LPET model. MLE provides point estimates while Bayesian analysis uses the full posterior distribution to capture uncertainty naturally. Comparative study of these two methods verified the stability of parameter estimates and assessed consistency. Bayesian posterior estimates closely matched the MLE estimates, confirming the robustness. The LPET model address the gap in parameter estimation using Bayesian method, validation using simulation, and application of the model on a real microcircuit failure data with comparisons to strong classical probability models. This study does not involve any clinical trial.

Emerging research prioritizes model order reduction methods and machine-learning solvers for verification [9]. The generalization of the probability models is studied in the major works [10] are major literature for custom probability models. Kumaraswamy Inverse exponential distribution [11], Inverse exponentiated Exponential Inverse [12]; Generalized Inverted Exponential distribution [13] are some generalized models using classical Exponential distribution. The Exponential Generalized Gamma distribution [14] is a four-parameter extension of generalized gamma distribution. One of the major applications of generalization is to get ability of fitting skewed and non-normal data available in modern practices [15]. Although these models have been effectively and significantly applied, they still fail to model diverse hazard shapes like bathtub and j-shaped. Classical parameter estimation methods like MLE, Cramer-Von Mises (CVM) and least square methods (LSE) are often insufficient for heavily tailed data with different hazard rate curves. Bayesian analysis for parameter estimation is a revolution [16] for getting more precise and accurate parameter for heavily tailed data having different hazard rate curves. Bayesian hypothesis testing expands the range of inferences that can be interpreted in intuitively [17]. The use of prior findings yields results in the form of an automatic meta-analysis [18,19]. Even for small sample, the Bayesian approach is less problematic.

Reliability analysis plays essential role in dealing with risks that arises from failure events [20,21]. Recent studies on electromigration in microcircuits include physics-based modeling [22], survival analysis for carbon fiber and electromigration [23]. Possible failures can lead to unexpected outcomes resulting injuries [24], deaths and environmental damage [25,26]. This study focusses on introduction of new probability generalization of exponential distribution, estimation of its parameters using Bayesian method, and applying on reliability data.

A large number of lifetime models are available in literature. Lehmann Type-I Exponentiation (Exponentiated-G family) modifies a baseline distribution cumulative distribution function (CDF) $F(x)$ to $F(x)^{\alpha}$ adding a shape parameter. Example include Exponentiated Exponential, Beta-Generalized distribution, EW and Exponentiated Gamma. The main advantages of these models are controlling skewness and flexibility in hazard function but still cannot produce both bathtub and inverted j shapes hazard jointly. The Power-transformed families (T-X families) use nonlinear transformations x^{λ} or $g(x)$ that alter the tail behaviors [10] but often fail to handle multimodal or non-monotone hazards without further extension. Mixed or compound models such as Lindley- and Beta-exponential enhance the performances of model but increase number of parameters yielding complex model with unstable estimation.

Several research gaps identified in available literature. No model simultaneously integrates Lehmann exponentiation and a power transformation together on x so that both shape and the failure rate accumulation. Many existing models fails to reproduce all five hazard shapes: increasing, decreasing, bathtub, j-shaped and inverted j-shaped. Also, Current literature lacks reliability model that can analyze microcircuit electromigration with multi-phase hazard behaviors.

This study addresses the gaps by proposing LPET model having following main innovations. The LPET model combines both Lehmann exponentiation and Power transformation of x, creating extra flexibility. Additional Frailty -like parameter α captures hidden heterogeneity and controls skewness. Similarly, Power parameter λ alters the growth rate. as well as model is highly flexible and may be able to control all major hazard rate shapes. Although the power transformations exist in other families like Weibull, using it in conjunction with exponentiation under this specific Exponential extension baseline creates an unexplored parameter space generating diverse hazard rate shapes.

This study introduces the novel probability distribution LPET demonstrating high flexibility in modeling various complex non-monotonic hazard shapes including j-shaped, bathtub and inverted j-shaped datasets in reliability study. through detailed simulation studies and the dual estimation process, the LPET model consistently outperforms classical as well as some new probability distributions. The robust Bayesian framework having excellent Markov chain Monte Carlo (MCMC) convergence ($\hat{R} = 1.00$) reveals consistent parameter estimates. The accurate reliability metrics offer engineers a very powerful tool for failure prediction as well as the maintenance management in electronic system.

The remainder of this paper is organized as follows. Section 2 includes theoretical foundation of the LPET distribution, its core statistical properties survival and hazard rate functions. Section 3 details the classical parameter estimation MLE method which supported by the simulation studies for evaluating the consistency of the estimator. Application to real- world data set, Profile likelihood function and model validation and comparison under classical approach. Section 4 incudes Bayesian frameworks, specifying prior distributions and posterior distributions using MCMC, adequacy model and sensitivity analysis of prior distributions. Section 5 include model validation encompassing convergence diagnostics, predictive performance checks as well as sensitivity analysis. Application of the model to a real-world microcircuit failure dataset, comparing the performances of LPET with competing distributions are included in this section. Section 6 is discussion which include details the key findings, highlighting the model's practical implications as well as the acknowledging the limitations of the study. Section 7 explain 'Declaration'. Finally, section 8 concludes with major contributions and suggestions for future research.

2. LPET Probability Distribution and Statistical Properties

This section presents the formulation of the introduced LPET distribution with some key properties, shape characteristics, as well as random number generation method. The LPET model is formulated by using two strong transformations: Lehmann Type-I exponentiation, and Power transformation of Baseline variable. These two transformations jointly formulate a very flexible probability model which can control diverse reliability patterns of modern reliability datasets.

2.1. *Model formulation*

This subsection of the study describes the formulation of the LPET model. The proposed LPET model is formulated to fulfill the limitations of standard exponentiated families introducing a power transformation x^{λ} with Lehmann exponentiation that allows separate control of early-life and wear-out phase. Let X follows the two-parameter exponential extension distribution [27] with CDF given in Eq. (1).

$$G(x,\lambda,\beta) = 1 - exp\left(-\lambda x e^{-\frac{\beta}{x}}\right),\ x > 0, (\lambda,\beta) > 0. \tag{1}$$

The corresponding probability density function (PDF) is:

$$g(x,\lambda,\beta) = \lambda\left(1+\frac{\beta}{x}\right)e^{-\frac{\beta}{x}}exp\left\{-\lambda x e^{-\frac{\beta}{x}}\right\}.\ \ x > 0, (\lambda,\beta) > 0 \tag{2}$$

Although, model (1) provides tail flexibility it does not capture the hazard rate patterns. To address this, two modifications are introduced in baseline model (1). First, Lehmann Exponentiation raises the CDF to a positive power $\alpha > 0$, i.e., $F(x) = [G(x)]^{\alpha}$. This enhances the distributional flexibility, controlling skewness, kurtosis and tail weight. Second, Power transformation of the baseline variable x as x^{λ} enhancing the rate of growth of failure probability. Together these transformations formulate LPET distribution.

It is important to clarify that, the parameter λ is introduced as a power parameter acting directly on x in proposed model LPET, unlike its role as a linear coefficient in the base Exponential Extension model which is taken as the baseline. This reparameterization is fundamental in probability modeling to enhancing the model's flexibility. The CDF and PDF obtained by modification introduce a novel probability distribution LPET with expression in Eqs. (3) and (4). The CDF function produce an adjustable growth rate, covering both slow and fast rising probability pattern.

$$F(x) = \left[1 - exp\left(-x^{\lambda}e^{-\beta/x}\right)\right]^{\alpha} \tag{3}$$

$$f(x) = \alpha x^{\lambda-1}e^{-\beta/x}\,exp\left(-x^{\lambda}e^{-\beta/x}\right)(\lambda+\beta x^{-1})\left[1 - exp\left(-x^{\lambda}e^{-\beta/x}\right)\right]^{\alpha-1} \tag{4}$$

Raising the entire original cdf to a power is a classical technique in statistics also known as the exponentiated *G* family. It is also called Lehmann Type I transformation which is a specific type of variance stabilizing transformation often used in statistics and plays very significant role in modeling the data sets. Parameter α is a frailty parameter capturing unobserved heterogeneity, while β and λ control spread, regulating the hazard shape and tails. The added parameter α controls the skewness, kurtosis as well as the tail behavior of the distribution. As we define $\alpha > 1$, model becomes more left-skewed and for $\alpha < 1$ model becomes more right skewed. This flexibility in the behavior of model allows it to fit a wider variety of real data sets. In reliability theory, α is interpreted as frailty or resilience parameter that accounts for unobserved heterogeneity in populations. The exponentiation plays very significant role to capture heavy tailed data generally used in finance, survival analysis and in hydrology.

Similarly, power-based scaling applied in modification of the original model control growth rate of the function x^{λ}. It helps in modeling in case of accelerated failure and growth pattern where rate of change is not linear. It also affects the hazard rate function. As λ becomes larger, it produces heavier tails, while a smaller λ creates lighter tails. Another significant impact of λ is structuring the different hazard rate curves. Survival/Reliability and hazard rate function of the LPET distribution are given in Eqs. (5) and (6). In reliability study, survival function shows probability of surviving beyond the time x. In proposed model LPET, both shot-lived and long-lived survival behaviors can be achieved.

2.2. *Survival function and hazard rate functions*

The survival function $S(x)$, which gives the probability that a unit services beyond time x, is given by Eq. (5)

$$S(x) = 1 - \left[1 - exp\left(-x^{\lambda}e^{-\beta/x}\right)\right]^{\alpha} \tag{5}$$

Hazard rate measures the instantaneous failure rate at time x is given by Eq. (6). Simpler models (e.g., exponential) hazard rate of LPET is highly flexible due to the adjustment and addition of parameters. These adjustments result in generating different shaped hazard rate curve such as increasing, decreasing, j- shaped, inverted j-shaped and bathtub curves.

$$h(x) = \alpha x^{\lambda-1}e^{-\beta/x}\, exp\left(-x^{\lambda}e^{-\beta/x}\right)\left(\lambda + \beta x^{-1}\right)\left[1 - exp\left(-x^{\lambda}e^{-\beta/x}\right)\right]^{\alpha-1}\left[1 - \left[1 - exp\left(-x^{\lambda}e^{-\beta/x}\right)\right]^{\alpha}\right]^{-1} \tag{6}$$

2.3. *Quantile function and random number generation*

Inverse transformation sampling method is appllied to derive quantile function $Q(p)$.The quantile function helps in random numbers generation from the model which maps a probability $p \in (0,1)$ to a value from distribution. Random samples can be obtained by putting random numbers into the quantile function given by Eq. (7). The main function of quantile function is to link probabilities to the data values. In LPET model quantile function effectively provides a way of simulating random samples.

Let U $\sim \mathrm{Uniform}(0,1)$. Then a random variable X which follows LPET distribution is obtained by $X \sim Q(U)$. The quantile function,

$$x^{\lambda}e^{-\beta/x} = -\,ln\left(1 - p^{1/\alpha}\right), p \in (0,1) \tag{7}$$

Since the Eq. (7) does not admit a closed-form solution of x, so quantile function must be evaluated numerically and are simulated using a numerical root finding Newton-Raphson method. The random deviate generating function is given by Eq. (8)

$$x^{\lambda}e^{-\beta/x} = -\ ln\left(1 -\ u^{1/\alpha}\right);\quad u \in U(0,1) \tag{8}$$

2.4. *Shape characteristics*

Fig. 1 demonstrates LPET's superior flexibility. Probability density plots at fixed beta ($\beta = 22$) (Left panel) and for different values of all three parameters. The density functions show that LPET can model both light-tailed as well a heavy tailed behavior. The PDF describes likelihood of distribution of observed value across the domain. For LPET, shapes of curve changes with parameters producing different shaped curves which makes model applicable where data deviate from normality.

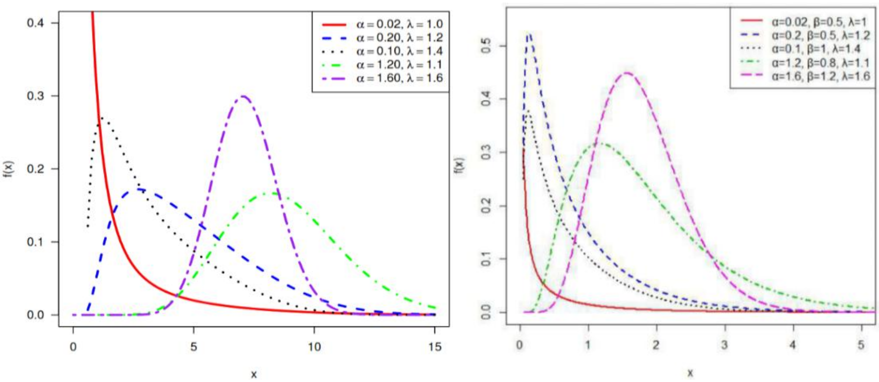

Fig. 1. Density plots of LPET model showing light-and heavy-tailed behaviors under different sets of parameters.

The hazard rate function of the LPET is given by (6) are displayed in Left panel (β = 22) and for different values of all three parameters in Right panel of Fig. 2. confirms that LPET's ability to capture bathtub, *j*-shaped and increasing that exponential and Weibull cannot capture and the hazard rate curves are bathtub, j-shaped, inverted *j*-shaped and inverted bathtub shaped.

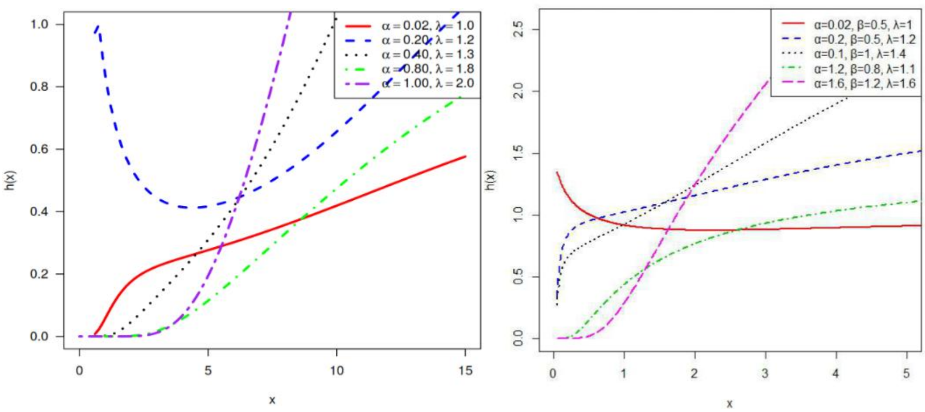

Fig. 2. Hazard rate plots illustrating *j*-shaped, inverted *j*-shaped, and bathtub forms, confirming flexibility beyond Weibull and Exponential distributions.

To understand the qualitative behaviors of LPET model, effects of two components diverse the LPET model as

(i) *Effects of Exponentiation parameter α (Frailty)*

$\alpha > 1$: heavier right tail, right skewed model; $\alpha = 1$: reduces to original (baseline exponential EE) Model; and for $\alpha > 1$: left-skewed, stronger central peak;

(ii) *Effects of power parameter λ*

Larger λ generates heavier tails, slow the failure accumulation and smaller λ generate lighter tails, faster risk accumulation.

2.5. *Skewness and kurtosis*

To study the consistency and normality of the data, Skewness and kurtosis were measured. Quantile based Bowley's skewness [28] and kurtosis [29] are;

$$S_k = \frac{Q(0.75) - 2Q(0.50) + Q(0.25)}{Q(0.75) - Q(0.25)}$$

and

$$K_u = \frac{Q(0.875) - Q(0.625) + Q(0.375) - Q(0.125)}{Q(0.75) - Q(0.25)}.$$

where, Q (.) is quantile functions of the model.

2.6. *Theoretical advantages over common exponentiated families*

The LPET is not merely a new member of the exponentiated-G family; it also introduces meaningful mathematical innovations to distinguish the model from important exponentiated model (EE) [5] as well as the EW [3]. Following unique properties of the proposed model are presented through formal propositions.

Proposition 1 (Quantile Function and Simulation Efficiency)

The quantile function defined by Eq. (7) admits no closed-form solution in terms of elementary functions. it can be effectively solved by using numerical method trough root-finding methods like Newton-Rapson due to monotonicity on left hand side. This contrasts with the exponentiated Exponential family where quantile is explicit and aligning with the EW family which also requires the numerical inversion.

Proposition 2 (Tail Behavior and Survival Asymptotic)

Using survival function defined in Eq. (5), as $x \to \infty\,; e^{-\beta/x} \to 1,$ so $x^{\lambda}e^{-\beta/x} \sim x^{\lambda}$, therefore, $exp(-x^{\lambda}e^{-\frac{\beta}{x}}) \sim e^{-x^{\lambda}}$ which decays to 0 very quickly. Also, for small y, $(1 - y)^{\alpha} \approx (1 - \alpha y)$. Also, let $y = exp(-x^{\lambda}e^{-\frac{\beta}{x}})$, here as $x \to \infty, y \to 0,$ thus $(1 - y)^{\alpha} \approx (1 - \alpha y)$. This implies;

$$S(x) = 1 - \left[1 - exp\left(-x^{\lambda} e^{-\beta/x}\right)\right]^{\alpha} = 1 - \left[1 - \alpha\, exp\left(-x^{\lambda} e^{-\beta/x}\right)\right]$$
$$= \alpha\, exp\left(-x^{\lambda} e^{-\beta/x}\right) \sim \alpha\, exp\left(-x^{\lambda}\right)$$

That is; as $x \to \infty$; $S\,(x) \sim \alpha\, exp(\,-\, x^{\lambda})$.

This implies that, tail decay is Weibull type with shape parameter λ and scale 1, heavier than exponential if λ < 1, and lighter than Exponential if λ > 1.

Also, $S_{EE}(x) \sim e^{-x}$ (exponential tail) and $S_{EW}(x) \sim e^{-x^{\gamma}}$ (Weibull tail with shape γ). The proposed model, LPET also have Weibull-type tail, but have also additional shape flexibility due to the $e^{-\beta/x}$term for small to moderate x, which EE and EW lack.

3. Classical Parameter Estimation

This study applied classical MLE and Bayesian analysis for parameter estimation of LPET distribution.

3.1. *Maximum likelihood estimation*

The loglikelihood function of the LPET is given in Eq. (9). Main contribution of loglikelihood function is to measure how well the parameters of the model fits the dataset.

$$\ell = n\, ln\, \alpha + (\lambda - 1)\sum_{i=1}^{n} ln x_i - \beta \sum_{i=1}^{n} \frac{1}{x_i} - \sum_{i=1}^{n} {x_i}^{\lambda} e^{-\beta/x_i} + \sum_{i=1}^{n} ln(\lambda + \beta {x_i}^{-1}) + (\alpha - 1)\sum_{i=1}^{n} ln\left[1 - exp\left(-{x_i}^{\lambda} e^{-\beta/x_i}\right)\right] \qquad (9)$$

Differentiating Eq. (9) with respect to unknown parameters and solving will give the estimated parameters. It is quite difficult to solve the equations. Newton-Raphson method can be used to solve these equations. Differentiating Eq. (9) partially with respect to parameter α, β, and λ;

$$\frac{\partial \ell}{\partial \alpha} = \frac{n}{\alpha} + \sum_{i=1}^{n} ln\left[1 - exp\left(-{x_i}^{\lambda} e^{-\beta/x_i}\right)\right],$$

$$\frac{\partial \ell}{\partial \beta} = \sum_{i=1}^{n} \frac{1}{x_i} + \sum_{i=1}^{n} {x_i}^{\lambda-1} e^{-\beta/x_i} + \sum_{i=1}^{n} \frac{1}{x(\lambda + \beta/x_i)} + (\alpha - 1)\sum_{i=1}^{n} \frac{{x_i}^{\lambda} e^{-\beta/x_i}\, exp\left(-{x_i}^{\lambda} e^{-\beta/x_i}\right)}{x_i\left[1 - exp\left(-{x_i}^{\lambda} e^{-\beta/x_i}\right)\right]}, \frac{\partial \ell}{\partial \lambda} = \sum_{i=1}^{n} ln\, x_i - \sum_{i=1}^{n} {x_i}^{\lambda}\, ln\, x_i\, e^{-\beta/x_i} + \sum_{i=1}^{n} \frac{1}{(\lambda + \beta/x_i)} \frac{1}{x_i} + (\alpha - 1)\sum_{i=1}^{n} \frac{{x_i}^{\lambda} e^{-\beta/x_i}\, ln\, x_i\, exp\left(-{x_i}^{\lambda} e^{-\beta/x_i}\right)}{\left[1 - exp\left(-{x_i}^{\lambda} e^{-\beta/x_i}\right)\right]}.$$

Similarly, second order partial derivatives are;

$$\frac{\partial^2 \ell}{\partial \alpha^2} = -\frac{n}{\alpha^2},$$

$$\frac{\partial^2 \ell}{\partial \beta^2} = \sum_{i=1}^{n}\left[\frac{{x_i}^{\lambda} e^{-\beta/x_i}}{{x_i}^2} - \frac{1}{{x_i}^2(\lambda + \beta/x_i)^2}\right] + (\alpha - 1)\sum_{i=1}^{n} \frac{{x_i}^{\lambda} e^{-\beta/x_i}\left(1 - {x_i}^{\lambda} e^{-\beta/x_i}\right) exp\left(-{x_i}^{\lambda} e^{-\beta/x_i}\right)}{x_i\left[1 - exp\left(-{x_i}^{\lambda} e^{-\beta/x_i}\right)\right]^2},$$

$$\frac{\partial^2 \ell}{\partial \lambda^2} = -\sum_{i=1}^{n} {x_i}^{\lambda}(ln x_i)^2 e^{-\frac{\beta}{x_i}} - \sum_{i=1}^{n}\left[\frac{1}{\left(\lambda + \frac{\beta}{x_i}\right)^2}\right] + (\alpha - 1)\sum_{i=1}^{n} \frac{{x_i}^{\lambda}\, ln x_i\, e^{-\beta/x_i}\, exp\left(-{x_i}^{\lambda} e^{-\beta/x_i}\right)\left({x_i}^{\lambda}\, ln x_i\, e^{-\beta/x_i} - 1\right)}{\left[1 - exp\left(-{x_i}^{\lambda} e^{-\beta/x_i}\right)\right]^2}.$$

Also, the cross partial derivatives with respect to parameter α, β, and λ are given as;

$$\frac{\partial^2\ell}{\partial\alpha\partial\beta} = \sum_{i=1}^{n} \frac{x_i{}^{\lambda} e^{-\beta/x_i} exp\left(-x_i{}^{\lambda} e^{-\beta/x_i}\right)}{x_i\left[1-exp\left(-x_i{}^{\lambda} e^{-\beta/x_i}\right)\right]},$$

$$\frac{\partial^2\ell}{\partial\alpha\partial\lambda} = \sum_{i=1}^{n} \frac{x_i{}^{\lambda} e^{-\beta/x_i}\, ln x_i\, exp\left(-x_i{}^{\lambda} e^{-\beta/x_i}\right)}{\left[1-exp\left(-x_i{}^{\lambda} e^{-\beta/x_i}\right)\right]},$$

$$\frac{\partial^2\ell}{\partial\beta\partial\lambda} = -\sum_{i=1}^{n} \frac{x_i{}^{\lambda}\, ln\, x_i\, e^{-\beta/x_i}}{x_i} - \sum_{i=1}^{n}\left[\frac{1}{x_i(\lambda+\beta/x_i)^2}\right] + (\alpha - 1)\sum_{i=1}^{n} \frac{x_i{}^{\lambda}\, ln\, x_i\, e^{-\beta/x_i}\, exp\left(-x_i{}^{\lambda} e^{-\beta/x_i}\right)\left(1 - x_i{}^{\lambda} e^{-\beta/x_i}(1+ln\, x_i)\right)}{x_i[1-exp(-x_i{}^{\lambda} e^{-\beta/x_i})]^2}$$

Estimation of unknown parameters $(\alpha,\ \beta, \lambda)$ can be performed by solving above single and double order partial derivatives (nonlinear equations) (25). As the equations are nonlinear, it will be quite rigorous in solving analytically. Newton- Raphson's iteration techniques was applied in log likelihood function of Eq. (9) using *optim()* function of R language programming. We have defined $\hat{\underset{\sim}{\delta}} = \left(\hat{\alpha}, \hat{\beta}, \hat{\lambda}\right)$ as MLE of $\underset{\sim}{\delta} = (\alpha, \beta, \lambda)^T$. Asymptotic normality result is $(\hat{\underset{\sim}{\delta}} - \underset{\sim}{\delta}) \to N_3(0, (I(\underset{\sim}{\delta}))^{-1}$ and fisher's information matrix $I(\underset{\sim}{\delta})$ is given by;

$$I(\underset{\sim}{\delta}) = -\begin{pmatrix} E\left(\frac{\partial^2\ell}{\partial\alpha^2}\right) & E\left(\frac{\partial^2\ell}{\partial\alpha\partial\beta}\right) & E\left(\frac{\partial^2\ell}{\partial\alpha\partial\lambda}\right) \\ E\left(\frac{\partial^2\ell}{\partial\beta\partial\alpha}\right) & E\left(\frac{\partial^2\ell}{\partial\beta^2}\right) & E\left(\frac{\partial^2\ell}{\partial\beta\partial\lambda}\right) \\ E\left(\frac{\partial^2\ell}{\partial\lambda\partial\alpha}\right) & E\left(\frac{\partial^2\ell}{\partial\lambda\partial\beta}\right) & E\left(\frac{\partial^2\ell}{\partial\lambda^2}\right) \end{pmatrix}$$

The MLE $\hat{\underset{\sim}{\delta}} = \left(\hat{\alpha}, \hat{\beta}, \hat{\lambda}\right)$ of $\hat{\delta} = (\alpha, \beta, \lambda)^T$was obtained using R programming language. It is important to note that MLE gives asymptotic variance $(I(\underset{\sim}{\delta}))^{-1}$. Approximation of the asymptotic variance can be done by taking estimated values of the parameters. For this Fisher's information matrix $O(\underset{\sim}{\delta})$ which is given as;

$$O(\underset{\sim}{\delta}) = -\begin{pmatrix} \frac{\partial^2\ell}{\partial\alpha^2} & \frac{\partial^2\ell}{\partial\alpha\partial\beta} & \frac{\partial^2\ell}{\partial\alpha\partial\lambda} \\ \frac{\partial^2\ell}{\partial\beta\partial\alpha} & \frac{\partial^2\ell}{\partial\beta^2} & \frac{\partial^2\ell}{\partial\beta\partial\lambda} \\ \frac{\partial^2\ell}{\partial\lambda\partial\alpha} & \frac{\partial^2\ell}{\partial\lambda\partial\beta} & \frac{\partial^2\ell}{\partial\lambda^2} \end{pmatrix} = -H(\underset{\sim}{\delta})|_{\underset{\sim}{\delta}=\hat{\underset{\sim}{\delta}}}$$. Here, H is the hessian.

The observed information matrix can be obtained by maximizing the likelihood. Newton Raphson algorithm is used to obtain the information matrix. Also, variance covariance matrix is

$$\left(-H(\underset{\sim}{\delta})|_{\underset{\sim}{\delta}=\hat{\underset{\sim}{\delta}}}\right)^{-1} = \begin{pmatrix} Var(\hat{\alpha}) & Cov(\hat{\alpha},\hat{\beta}) & Cov(\hat{\alpha},\hat{\lambda}) \\ Cov(\beta,\alpha) & Var(\hat{\beta}) & Cov(\hat{\beta},\hat{\alpha}) \\ Cov(\hat{\lambda},\hat{\alpha}) & Cov(\hat{\lambda},\hat{\alpha}) & Var(\hat{\lambda}) \end{pmatrix}$$

Hence from asymptotic normality of MLE approximate $100(1-\gamma)$ % confidence interval (CI) for the parameters were calculated using upper percentile standard normal variate.

$$\hat{\alpha} \pm z_{\gamma/2}\sqrt{v\ a\ r(\hat{\alpha})}, \hat{\beta} \pm z_{\gamma/2}\sqrt{v\ ar(\hat{\beta})} \text{ and } \hat{\lambda} \pm z_{\gamma/2}\sqrt{v\ a\ r(\hat{\lambda})}$$

where $z_{\gamma/2}$ is the upper percentile of standard normal variate.

3.2. *Simulation study*

In case of analytical results, study become very complex more often when formula for descriptive measures do not have closed form solutions. Simulation is alternative way to study the behavior of the distribution. Simulation repeatedly generates random samples from model considered and important characteristics such as bias, root mean squared error (RMSE), root mean square error and convergence are measured which give detailed insights to know how well the model and estimates perform.

Bias is the average deviation of estimator from true parameter while mean squared error (MSE) uses both variances and bias to give average squared distance between the estimate and true value. Smaller value of MSE indicate more consistent estimates across replications. Lower value of RMSE which is square root of MSE indicate higher precision and better estimator performances.

Numerical optimization algorithm in Monte Carlo replication was supposed to have converged if optimizer status, change in log-likelihood (LL) and change in parameter vector considered numerically stable. For every Monte- Carlo replication, monitoring of the consistency of both LL values and parameter values given by optimization routine needs for convergence measurement.

Let, $\theta^k = \left(\alpha^{(k)}, \beta^{(k)}, \lambda^{(k)}\right)$ is the parameter vector at k^th^ iteration and also let $L^{(k)} = L\left(\theta^{(k)}\right)$ be the corresponding LL value then convergence can be measured by checking (i) the maximization routine (BFGS) returned a successful convergence code = 0, (ii) change in LL< $10^{-6}$and (iii) maximum update for parameter below 10^{-6}. In addition of Bias, MSE, and RMSE, we also evaluated convergence rate which is the ratio of the number of converged replications to the total number of replications.

That is, $\text{Convergence Rate} = \frac{\text{Number of converged replications}}{\text{Total number of replications}}$.

A convergence rate close to $1(>\ 0.95)$ is supposed that optimization procedure is stable.

3.2.1. *Simulation design*

To evaluate the finite-sample performance of MLEs, we conducted Monte Carlo simulations recommended in literature [30] including MSE, RMSE and bias as accuracy metrices. The study generates samples under three parameter sets for assessing bias, MSE, RMSE, and convergence rates across $n\ =\ 100$ to 1000. Monitoring of optimization convergence is assessed via BFGS and parameter change thresholds. Bias, MSE, and RMSE of parameter estimate across increasing sample sizes for three parameter sets are shown in

Tables 1-3. For example, parameter set ($\alpha = 2, \lambda = 2, \beta = 1.5$), bias reduced from (1.0427, 0.1555, 0.2798) at n = 100 to (0.0858, 0.0152, 0.02780) at n = 1000. Simulation study Tables 1-3 were computed using all the converged replications among the 1000 runs.

Table 1. Simulation study for α = 0.5, λ = 1, β = 0.5.

	Bias			MSE			RMSE			
n	α	λ	β	α	λ	β	α	λ	β	Convergence Rate
100	0.0018	0.0470	0.2312	0.0443	0.0240	0.4786	0.2105	0.1549	0.6918	0.8170
200	-0.0075	0.0225	0.1413	0.0257	0.0103	0.2328	0.1604	0.1013	0.4825	0.8900
300	-0.0049	0.0146	0.0840	0.0171	0.0064	0.1173	0.1308	0.0801	0.3426	0.8990
400	-0.0105	0.0090	0.0891	0.0158	0.0041	0.1066	0.1257	0.0637	0.3265	0.9010
500	-0.0060	0.0026	0.0617	0.01140	0.0031	0.0670	0.1067	0.0561	0.2588	0.9200
600	-0.0014	0.0070	0.0484	0.0108	0.0025	0.0589	0.1041	0.0504	0.2427	0.9500
700	-0.0065	0.0012	0.0466	0.0087	0.0020	0.0454	0.0935	0.0452	0.2129	0.9360
800	-0.0094	0.0048	0.0505	0.0079	0.0019	0.0430	0.0889	0.0435	0.2073	0.9360
900	-0.0065	0.0052	0.0350	0.0067	0.0018	0.0289	0.0817	0.0428	0.1700	0.9390
1000	-0.0068	0.0037	0.0397	0.0068	0.0016	0.0355	0.0823	0.0398	0.1884	0.9440

Note: Convergence Rate = Number of Converged replications / 1000

Table 2. Simulation study for α = 1.5, λ = 1.5, β = 1.

	Bias			MSE			RMSE			
n	α	λ	β	α	λ	β	α	λ	β	Convergence Rate
100	0.2007	0.1712	0.5766	1.3601	0.1669	2.7818	1.1662	0.4086	1.6679	0.9930
200	0.2749	0.0801	0.2407	1.2032	0.0488	1.1119	1.0969	0.2209	1.0545	0.9990
300	0.2438	0.0643	0.2069	1.0844	0.0352	0.8886	1.0413	0.1877	0.9427	1.0000
400	0.2574	0.0413	0.1101	0.9869	0.0193	0.5767	0.9934	0.1389	0.7594	1.0000
500	0.2379	0.0395	0.1080	0.9494	0.0170	0.5289	0.9744	0.1304	0.7273	1.0000
600	0.2740	0.0274	0.0389	0.8698	0.0133	0.4406	0.9326	0.1152	0.6638	1.0000
700	0.2623	0.0169	0.0097	0.7860	0.0098	0.3570	0.8865	0.0992	0.5975	1.0000
800	0.2493	0.0149	0.0134	0.7642	0.0087	0.3406	0.8742	0.0930	0.5836	1.0000
900	0.2576	0.0151	0.0008	0.7596	0.0083	0.3206	0.8716	0.0910	0.5662	1.0000
1000	0.2406	0.0158	0.0082	0.7282	0.0078	0.3119	0.8534	0.0884	0.5585	1.0000

Note: Convergence Rate = Number of Converged replications / 1000

Table 3. Simulation study for α = 2, λ = 2, β = 1.5.

	Bias			MSE			RMSE			
n	α	λ	β	α	λ	β	α	λ	β	Convergence Rate
100	1.0427	0.1555	0.2798	7.4637	0.2920	2.6677	2.7320	0.5404	1.6333	1.0000
200	0.5703	0.0730	0.1300	3.7165	0.0868	0.9969	1.9278	0.2946	0.9984	1.0000
300	0.4192	0.0372	0.0528	2.2488	0.0518	0.6443	1.4996	0.2277	0.8027	1.0000
400	0.2857	0.0345	0.0596	1.5542	0.0386	0.4741	1.2467	0.1965	0.6885	1.0000
500	0.2312	0.0222	0.0310	1.1420	0.0289	0.3647	1.0686	0.1701	0.6039	1.0000
600	0.2415	0.0150	0.0155	1.1205	0.0247	0.3363	1.0586	0.1572	0.5799	1.0000
700	0.1883	0.0191	0.0234	0.8614	0.0218	0.2900	0.9281	0.1476	0.5385	1.0000
800	0.1551	0.0115	0.0133	0.5525	0.0190	0.2451	0.7433	0.1377	0.4951	1.0000
900	0.1234	0.0108	0.0122	0.4429	0.0166	0.2057	0.6655	0.1290	0.4536	1.0000
1000	0.0858	0.0152	0.0278	0.3622	0.0139	0.1758	0.6018	0.1178	0.4193	1.0000

Note: Convergence Rate = Number of converged replication / 1000

Bootstrap CIs were attempted and were found not stable due to flat likelihood regions in resampled data which is very common issue in three- parameter lifetime models.

Bias and MSE consistently reduces across all parameters as *n* increases demonstrating the better estimator consistency. The convergence rate mentioned in table of simulation indicate proportion of 1,000 replications converged successfully.

Fig. 3 demonstrates plot of bias and RMSE versus sample size. As sample size increase from 100 to 1000 both bias and MSE decreased substantially. That is, both bias and RMSE decrease steadily as sample size increases across all parameter sets. With Set 1 showing the best overall performance and Sets 2-3 exhibiting higher error mainly at smaller sample sizes. This confirms the consistency of the estimators.

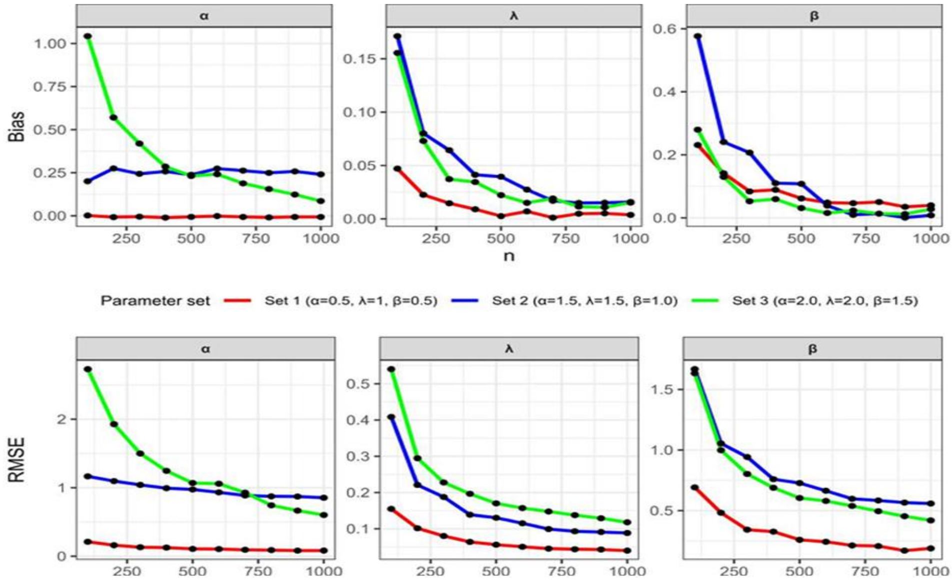

Fig. 3. Plots of Bias, RMSE, and Convergence vs Sample Size.

Table 4 demonstrate the better simulation performance with 35-97 % lower MSE as well as 23-86 % lower bias with respect to Weibull, lognormal and exponential distribution and maintain good convergence rates for sample sizes ≥ 500.

Table 4. Monte Carlo Simulation and Improvement.

Metric	Set1(α=0.5, λ=1, β=0.5)	Set 2 (α=1.5, λ=1.5, β=1)	Set 3 (α=2, λ=2, β=1.5)
Sample size(n)	500	500	500
LPET Bias	0.02	0.13	0.09
LPET MSE	0.03	0.50	0.51
Weibull Bias	0.142	0.215	0.58
Weibull MSE	0.709	1.102	2.78
Exponential Bias	0.089	0.167	0.1245
Exponential MSE	0.789	1.178	0.789
Lognormal Bias	0.11	0.185	0.32
Lognormal MSE	0.65	0.95	1.85

LPET Conv. Rate	0.92	1.00	1.00
Bias Improv. vs Weibull	6.34 %	40.25 %	83.56 %
MSE Improv. vs Weibull	96.17 %	54.77 %	81.60 %
Bias Improv. vs Exponential	78.20 %	23.07 %	23.86 %
MSE Improv. vs Exponential	96.56 %	57.69 %	35.12 %

3.3. *Application to real-world data sets using classical method*

To check the practical applicability of the LPET, we have applied it on a real dataset from an accelerated life test that includes 59 conductors [31,32] where failure time is measured in hours with no censoring of the observations. The data include electromigration occurred in circuit due to failures in microcircuit by movement of atoms in the circuits.
4.700, 6.545, 9.289, 7.543, 6.956, 6.492, 5.459, 8.120, 4.706, 8.687, 2.997, 8.591,6.129, 11.038, 5.381, 6.958, 4.288, 6.522, 4.137, 7.459, 7.495, 6.573, 6.538,5.589, 5.807, 6.725, 8.532, 9.663, 6.369, 7.024, 8.336, 9.218, 7.945,6.869, 6.352, 6.087, 6.948, 9.254, 5.009, 7.489, 7.398, 6.033, 10.092, 7.496, 7.974, 8.799, 7.683, 7.224, 7.365, 6.923, 5.640, 5.434, 7.937, 6.515, 6.476, 6.071, 10.491, 5.923 ,4.531.

All the numerical analysis and the graphics are performed using the R software [33]. The moment Package in R is used to calculate the skewness and kurtosis of the dataset. A descriptive study of the data was conducted; summary statistics are obtained and given in Table 5. Summary statistics describes the characteristics of the distribution providing deeper insights into its adaptability in different data formats. Summary statistics indicated that data are positively skewed and non-normal in nature.

Table 5. Summary statistics.

Minimum	Q_1	Q_2	Mean	Q_3	Maximum	SK	Kurtosis
2.997	6.052	6.923	6.980	7.941	11.038	0.193	3.087

Estimated parameters using MLE and corresponding Standard error of estimates and 95 % credible limits are presented in Table 6.

Table 6. Estimated parameters, standard error of estimates and 95 % credible Interval.

Parameters	Estimates	Standard Errors	CI	z-value	p-value	Significant
Alpha	1.058	0.629	(-0.177, 2.290)	1.682	0.092	
Beta	22.261	8.967	(4.650, 39.806)	2.483	0.013	*
Lambda	1.500	0.352	(0.811, 2.191)	4.261	<0.001	***

Note: *$p < 0.05$, **$p < 0.01$, **$p < 0.001$

Parameter β is the dominant driver of microcircuit failure behaviors, λ provides captures nonlinear effects and provides flexibility while α may not affect strongly (Under MLE) in this dataset but may affect strongly on other datasets.

For particular dataset, shape parameter α may not provide a statistically significant improvement in fit but the LPET model remains theoretically useful since α may allow for greater flexibility in shape and tail behavior in other sets of data.

3.4. *Profile likelihood functions*

A profile likelihood function was obtained using maximizing the loglikelihood function for all parameters except the one which is of interest varying the parameter across a grid of values. For a parameter θ, the profile likelihood may be defined as;

$$L_p(\theta) = \underbrace{maxL}\, L(\theta, \omega),$$

where, ω represents all other parameters. Each curve in Fig. 4 displays the profile likelihood for α, β, and λ. The peak of curve corresponds the MLE and the curvature around the peak indicate the sensitivity of likelihood to change in the particular parameter value. flatter curve indicates lower precision while steeper curve indicates the higher precision with lower standard error.

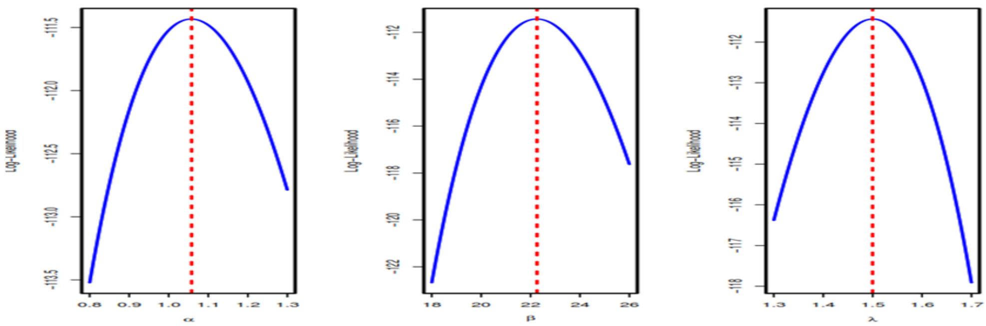

Fig. 4. Profile plots of the parameters.

The horizontal line is plotted at $L_p(\hat{\theta}) - \frac{1}{2}\chi^2_{1,0.95}$ provided the approximate 95 % CI for the parameter. Lower and upper limits confidence interval are the points where the profile curve intersects this line.

The profile likelihood curves for α, β, and λ were constructed by fixing each parameter using likelihood cutoff

$$L(\theta) \geq L_p(\hat{\theta}) - 1.92$$

Corresponding to a chi- square distribution (1 df) and the 95 % confidence interval were obtained as α ϵ (0.3772, 3.000), β ϵ (8.5443, 40.000) and λ ϵ (1.0063, 2.4937).

3.5. *Model validation comparisons under classical approach*

To check the graphical to goodness of fit, probability vs probability(P-P) and Quantile vs Quantile(Q-Q) plots are plotted and displayed in Fig. 5. Plots shows that the LPET model fits the data more precisely.

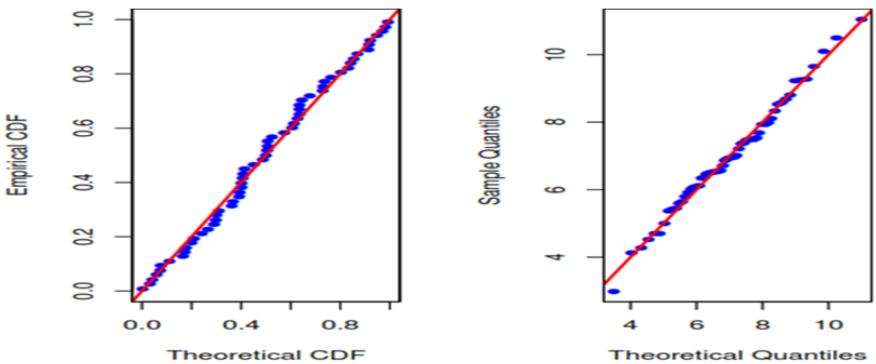

Fig. 5. P-P plot(left) and Q-Q plot (right) of LPET distribution.

To verify the superiority of the LPET model is compared with elven other models found in literature. The LL, Akaike Information Criterion (AIC), Bayesian Information Criterion (BIC), Consistent Akaike Information Criterion (CAIC), Hannan-Quinn Information Criterion (HQIC), Kolmogorov-Smirnov (KS) Statistic and corresponding p value are used for model comparison. LL measures how well a statistical model fits the observed data and the higher the LL value indicate model assigns greater probability to that data. AIC penalizes models with more parameters to avoid overfitting and lower AIC is preferred. BIC put high penalty for additional parameters and favors the model with lower BIC value. Similarly, CAIC is modified form of AIC even stronger penalty for model complexity and prefer model with lower CAIC. HQIC penalizes parameters heavier than AIC and lighter than BIC with lower value to prefer a model. KS test statistics compare empirical and theoretical cdf. The smaller KS and larger p-value mean good fit. Also, *p*-value more than 0.05 indicate not rejection and less than 0.05 indicates the rejection of the model.

The competitive models are Cauchy Modified Inverse Gompertz [34], Weibull Distribution, Weibull Extension (WE) Model [35], Lognormal, Kumaraswamy-Half-Cauchy (KSHC) distribution [36], Exponentiated-Exponential (EE) model [5], Lindley-Exponential (LE) model [37], Exponential Power (EP) model [38], Modified Weibull (MW) Model [39], Beta Exponential (BE) distribution [40] and Exponential distribution. Under MLE estimation method, information criteria and to test the goodness of fit, Kolmogorov Smirnova test statistics with p values are presented in Table 7. Least values of information criteria AIC (228.87) and maximum of p-values (0.946) confirm the excellent fit of the LPET model among the competitive model.

Table 7. LL, Information criteria and KS statistics with *p* values using MLE.

Distribution	LL	AIC	BIC	CAIC	HQIC	KS	*p*-value
LPET	-111.432	228.865	235.098	229.302	231.299	0.066	0.946
CMIG	-111.259	230.518	238.828	231.259	233.762	0.053	0.993
Weibull	-112.497	228.995	233.150	235.150	230.617	0.096	0.616
WE	-112.505	231.011	237.243	231.447	233.444	0.096	0.609
Lognormal	-112.971	229.942	234.097	236.097	231.563	0.087	0.734

KSHC	-114.668	233.337	237.492	239.492	234.959	0.101	0.548
EE	-114.947	233.895	238..050	234.109	235.517	0.104	0.510
LE	-114.953	233.906	238.061	234.120	235.528	0.104	0.510
BE	-114.955	233.910	238.066	240.066	235.532	0.1040	0.513
EP	-116.502	237.003	241.158	237.209	238.625	0.137	0.202
MW	-117.352	240.704	246.937	241.140	243.137	0.135	0.216
Exponential	-173.641	349.281	351.359	352.359	350.092	0.430	0.000

4. Bayesian Analysis of LPET Model

In this section, Bayesian analysis of the LPET model with other important studies are included. MLE method of parameter estimation misestimate parameters if sample size is small or skewed. Bayesian analysis provides efficient sampling and stable posterior distribution with credible interval capturing uncertainty fully.

4.1. *Bayesian framework*

Let x = (x_1, …, x_n) be a random sample from LPET distribution with parameters $\alpha > 0$, $\beta > 0$, $\lambda > 0$. The PDF is

$$f(x|\alpha,\lambda,\beta) = \alpha x^{\lambda-1}e^{-\beta/x}\, exp\left(-x^{\lambda}e^{-\beta/x}\right)(\lambda+\beta x^{-1})\left[1-exp\left(-x^{\lambda}e^{-\beta/x}\right)\right]^{\alpha-1}$$

The corresponding LL is

$$L(\alpha,\lambda,\beta|x) = n\, ln\,\alpha + (\lambda-1)\sum_{i=1}^{n} lnx_i - \beta\sum_{i=1}^{n}\frac{1}{x_i} - \sum_{i=1}^{n} {x_i}^{\lambda}e^{-\beta/x_i} + \sum_{i=1}^{n} ln(\lambda + \beta {x_i}^{-1}) + (\alpha-1)\sum_{i=1}^{n} ln\left[1-exp\left(-{x_i}^{\lambda}e^{-\beta/x_i}\right)\right]$$

This likelihood is used for both classical and Bayesian estimations (Eq. 9). Due to the nonlinear form, closed-form solution for the MLEs do not exist, hence numerical as well as Bayesian simulation are required.

4.2. *Main priors for Bayesian estimation*

This study uses four priors; one for the main Bayesian analysis and other three priors are used for checking the robustness of the priors. The main Bayesian analysis use the normal priors. Since all three parameters of the LPET model are strictly positive, so to enforce positivity we specify independent informative prior distributions on logarithm scale and improve sampling efficiency.

$$log(\alpha) \sim N(0,1), log(\beta) \sim N(0,2), log(\lambda) \sim N(0,1).$$

On original scales, the prior densities obtained are

$$\pi(\alpha) = \frac{1}{\alpha\sqrt{2\pi}} exp\left(-\frac{1}{2}(log\,\alpha)^2\right);$$

$$\pi(\beta) = \frac{1}{\beta\sqrt{4\pi}} exp\left(-\frac{1}{4}(log\,\beta)^2\right),$$

$$\pi(\lambda) = \frac{1}{\lambda\sqrt{2\pi}} exp\left(-\frac{1}{2}(log\,\alpha)^2\right).$$

The joint prior distribution which is product of the independent marginal priors is given as

$$\pi(\theta) = \pi(\alpha)\pi(\beta)\pi(\lambda).$$

Here, independent log-scale priors were used because all the parameters of the LPET model must be positive as well as to improve the sampling accuracy, preventing chains to entering invalid parameter region and stability. These priors act as the main priors which is used for Bayesian estimations. This main prior is used for; Posterior means and credible interval, LOO/WAIC model comparison, for predictive checks and convergence diagnostic (R-hat, ESS)

4.2.1. *Justification of the main priors*

The following are the main consideration for the choice of these priors
All the three parameters of the LPET model are positive so log-normal transformation of parameters and placing Gaussian priors on log(θ) ensures strictly positive without truncation. furthermore, the variances (1-2) are enough broad that will avoid imposing strong prior beliefs and will allow likelihood to dominate the posterior distribution. Also, Log-scale priors improve sampling efficacy and consequently prevent the Markov chains from exploring unstable region yielding better mixing along with more reliable posterior summaries. Finally, these prior helps model to adopt wide range which are highly applicable for lifetime models as well as generalized failure time distribution [41, 42] under minimum domain knowledge.

4.3. *Posterior distribution*

Assuming the independencies among the priors, the joint posterior distribution is proportional to the product of likelihood and joint prior distribution and is given as

$$\pi(\theta|x) \propto L(\theta/x)\pi(\theta).$$

Hence substituting likelihood and prior the posterior distribution becomes as (Eq.10)

$$\pi(\alpha,\beta,\lambda|x) \propto L(\theta/x)\pi(\theta).$$

The joint posterior distribution is therefore

$$\pi(\alpha,\beta,\lambda|x) \propto \left[\prod_{i=1}^{n} \alpha x_i^{\lambda-1} e^{-\beta/x_i}\, exp\left(-x_i^{\lambda} e^{-\beta/x_i}\right)(\lambda+\beta x_i^{-1})\left[1 - exp\left(-x_i^{\lambda} e^{-\beta/x_i}\right)\right]^{\alpha-1}\right]\pi(\alpha)\pi(\beta)\pi(\lambda). \tag{10}$$

4.4. *MCMC sampling scheme and convergence assessment*

Hamiltonian Monte Carlo (HMC) with No-U-Turn Sampler (NUTS) was used for posterior computation. This study uses MCMC techniques for estimation of parameters. Stan (cmdstanr or rstan) was used for Hamiltonian Monte Carlo (HMC and JAGS via rjags for Metropolis-Hastings (MH).Convergence was assessed using trace plots, effective sample size as well as Gelman-Rubin $\hat{R}$ indicating good mixing as nearly$\hat{R} = 1.00$. Alternative MCMC algorithms, such as the metropolis-within-Gibbs [43] for joint longitudinal and survival data were also used for robustness checks. We implemented the Metropolis-Hastings algorithm that uses a Gaussian random walk proposal distribution because each parameter of LPET distribution was updated using a normal proposal which was centered at its current value. The MH sampler was also used for comparison and to verify the robustness of Bayesian estimates.

4.4.1. *MCMC implementation steps*

We ran four MCMC chains of Hamiltonian Monte Carlo (HMC) with No-U-Turn Sampler (NUTS), each with 50000 iterations (10000 warm-up, thinning every 5th sample), resulting in 8,000 post warmup draws per chain and 32000 total posterior draws.

Convergence is assessed via $\hat{R} < 1.00$ and ESS > 2000, trace plots, and autocorrelations. Mean survival time (MTTF=7.126) as well as median survival time (MTTF50=7.075) are reported. Kaplan-Meier survival curve is plotted and compared with LPET fitted survival curve.

4.5. *Priors for sensitivity analysis*

To evaluate the robustness of the Bayesian inferences, the study is repeated for the analysis under three alternative priors:
Gamma (shape =2) - Moderately informative; Gamma (shape=1) – weakly informative and Lognormal – alternative positive prior on original scale. The use of gamma priors for Bayesian estimation of lifetime parameters has been validated under various loss functions [44].

4.5.1. *Justification for sensitivity priors*

Gamma (2,1) provides moderate concentration allowing flexibility. Gamma (1,1) is weakly informative baseline prior. Similarly, Lognormal produce heavier tail and allow assessment of sensitivity to tail behaviors and Hyperparameters were centered using empirical bayes approach. that is, the robustness of Bayesian inferences to prior specification is assessed by conducting a sensitivity analysis comparing three different priors' formulation. These are; Gamma (2,1), Gamma (1,1) and Lognormal distribution. Prior sensitivity analysis is important for verifying that posterior inferences are not unduly influenced by prior specification. In Bayesian Modeling, model specification and prior choices affect Bayesian hypothesis tests, underscoring the importance of rigorous sensitivity checks [45].

Using empirical bayes approach, informative priors were chosen. The MLE for all parameters were obtained using the real data set which were used as the prior means for the parameters. Gamma prior with moderate shape parameters were chosen for reasonable dispersion. A prior sensitivity analysis was conducted taking informative gamma, weakly informative Gamma and Lognormal priors

4.6. *Posterior summaries*

4.6.1. *Parameter estimation using Bayesian approach*

Posterior parameter summary of Bayesian analysis shown in Table 8. posterior summaries based on four chains with 50000 iterations each, discarding the first 10,000 warmup and thinning every 5th iteration (post-warmup draws per chain of 8000, 32000 total). Model implemented in stan 2.32.0 with cmdstanr 0.6.1 interface

The 2.5 %, 25 %, 50 %, 75 % and 97.5 % values correspond to posterior quantiles obtained from the MCMC sample. The 2.5 % and 97.5 % quantiles give the 95 % Bayesian credible interval while shape and spread of the posterior distribution can be defined using 25 %, 50 % and 75 % quantiles. the 50% quantile describe the posterior median.
Also, since all the parameters exhibited excellent convergences as for all parameters potential scale reduction factors ($\hat{R}$) of 1 with effective sample size vastly increasing from threshold of 1000, so MCMC chains characterized the posterior distribution reliably.

Table 8. Posterior parameter summary.

	Mean	SE	SD	2.5 %	25 %	50 %	75 %	97.25 %	ESS	R-hat
alpha	1.13	0.01	0.40	0.56	0.85	1.06	1.33	2.12	2364.00	1.00
beta	22.40	0.12	5.24	13.55	18.69	21.98	25.50	33.87	2072.00	1.00
lambda	1.50	0.00	0.22	1.30	1.34	1.48	1.62	1.97	2251.00	1.00

Table 9 displays the MLE vs Bayesian Posterior means and the 95% confidence interval. Results shows that there is high consistency in the estimates by both the methods. This supports the robustness of the methods.

Table 9. MLE vs Bayesian Posterior Means.

Parameter	MLE	95 % CI	Bayesian Mean	95 % CI
alpha	1.058	(-0.177, 2.290)	1.130	(0.56, 2.12)
beta	22.261	(4.650, 39.806)	22.464	(13.55, 33.87)
lambda	1.500	(0.811, 2.191)	1.498	(1.30,1.97)

4.7. *Model adequacy*

4.7.1. *Leave-One-Out cross-validation and widely applicable information criterion*

Furthermore, Leave-One-Out cross-validation (LOO) and the Widely Applicable Information Criterion (WAIC) which are the modern tools of Bayesian Model Comparisons for sample predictive accuracy [46,47]. These tools are based on LL evaluated at the posterior distribution are used. Expected Log Predictive Density-LOO(ELPD-LOO) measures predictive accuracy using approximate leave-one-out cross-validation and the less negative values indicate better predictive performance. p-loo (Effective number of parameters used by LOO) represents model complexity estimated by LOO cross- validation similar to AIC/ BIC with larger value indicating more flexible model [41]. LOOIC (Leave-One-Out Information Criterion) and WAIC are information criteria where lower values represent better predictive performance. Also, p-waic (Effective number of parameters under WAIC) with larger value indicates more flexible model.

Bayesian model comparison for ELPD-LOO and ELPD-WAIC are the expected log predictive densities displayed in table 10. LOO and WAIC with higher values (less negative) indicate the better predictive accuracy of the model. The almost equal values of LOO and WAIC suggests the consistency between both the estimation methods. Furthermore, p-LOO (2.27) and p-WAIC (2.24) which represents the effective number of parameters used by model are very close to 2.2 indicating that model is not overfitting. That is, LPET model is simple compared to the sample size. Also, both the LOOIC (227.56) and WAIC (227.50) are very close and smaller confirming model conformances by both the methods.

Table 10. Bayesian model comparison.

Measure	Elpd-loo	p-loo	looic	Elpd-waic	p-waic	waic
Value	-113.78	2.27	227.56	-113.75	2.24	227.50

4.8. *Sensitivity analysis*

Sensitivity to priors was tested using Gamma (2,1), Gamma (1,1), and Lognormal priors to evaluate the robustness of Bayesian estimate. Table 11 displays posterior summaries for all tree parameters (α, β, λ) appears highly consistent across different priors with minimal variations. Also, the prior sensitivity analysis reveals that R-hat approximately equal to 1 ($R < 1.05$) with effective sample sizes (ESS) 275-557 for all the parameters demonstrated excellent convergences for all the models and also confirms that final inference is not influenced by the choice of prior conforming robustness of Bayesian model. Results of sensitivity analysis show minimal variation in posterior means, confirming robustness.

Table 11. Sensitivity analysis for prior distribution and diagnostics.

Prior	Parameter	Mean	SD	Median	2.5 %	97.5 %	R-hat	ESS
Gamma	α	1.155	0.496	1.06	0.474	2.368	1.007	450
(shape=2)	β	22.754	6.496	21.894	12.568	37.98	1.011	453
	λ	1.508	0.26	1.476	1.099	2.117	1.01	557
Gamma	α	1.239	0.654	1.084	0.438	2.911	1.018	312
(shape=1)	β	22.545	7.563	21.505	10.961	40.21	1.011	339
	λ	1.501	0.297	1.459	1.043	2.188	1.009	422
Lognormal	α	1.233	0.657	1.07	0.439	2.958	1.008	275
	β	22.753	7.758	21.771	10.988	40.331	1.018	350
	λ	1.51	0.305	1.471	1.043	2.211	1.016	413

5. *Model Validation Framework*

5.1. *Trace plots for the parameters*

Trace plots for parameters are shown in Fig. 6. The plots shows that the trace plots using Bayesian MCMC estimation has good mixing and convergences across chains, which supports reliability of Bayesian parameter estimates.

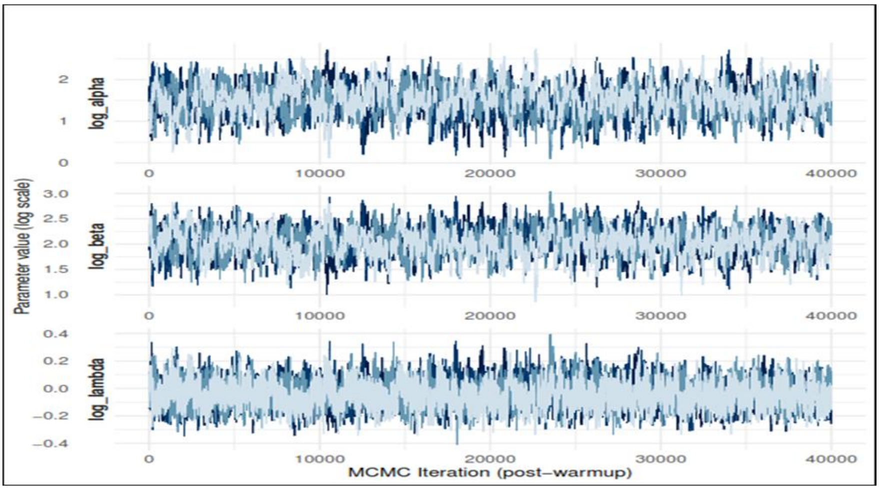

Fig. 6. Trace plots showing chain mixing of LPET model.

Fig. 7 shows the marginal posterior density plots with 95 % Credible interval of all parameters using eight MCMC chains. The curves from all chains overlap closely indicating excellent chain convergence. Plots shows that posteriors are unimodal and good mixing.

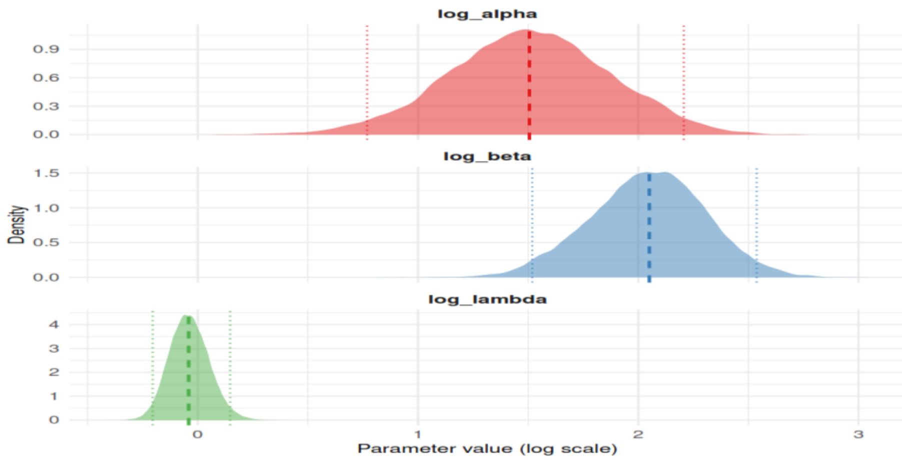

Fig. 7. Marginal posterior density plots with 95 % Credible Interval of LPET distributions.

Model Validation framework consists of following multifaceted approach. This will clarify the robust MCMC convergence.

5.2. *Convergence assessment*

The Gelman-Rubin diagnostic [48] which is also known as the potential scale Reduction Factor (PSRF) denoted by $\hat{R}$ is also analyzed. The PSRF is widely used convergence measure in MCMC estimation. It compares the within chain variability to the between chain variability of multiple Markov Chain Monte Carlo estimation in Bayesian analysis. The $\hat{R}$ < 1.01 indicates the excellent convergence and $\hat{R}$< 1.1 indicates adequate convergence.

Gelman-Rubin Diagnostics is computed for all three parameters using 4 parallel chains having threshold of $\hat{R}$< 1.05, all parameters meet these criteria (Table 12). Also, chains exhibited max $\hat{R}$=1 as excellent agreement. Trace plot inspection (Fig. 4) shows stationary and mixing as well as the chains seems to converges rapidly having no drifts post-burn-in. Multivariate PSRF is 1 and the effective sample sizes are α = 2510, β = 2802 and λ = 7070.

Table 12. Potential scale reduction factors.

Parameters	Point Est.	Upper C.I.
alpha	1	1
beta	1	1
lambda	1	1

Fig. 8 displays the autocorrelation of LPET distribution. All the parameter α, β and λ show rapid decay in autocorrelation approaching to zero within first few lags indicating good mixing as well as efficient sampling for the parameters, lambda shows more persistence in autocorrelation but still decays to zero within certain lags. Analysis suggests efficient sampling for all the parameters as it decayed below the 95 % confidence threshold within 10 lags. This supports the model applicability for conductor failure data and satisfactorily mixing of all three parameters.

5.3. *Predictive performance*

5.3.1. *Test for goodness of fit*

Information criteria and goodness of fit for model validation are analyzed. Bayesian estimation exhibits AIC =228.87, BIC = 235.10, CAIC = 238.10 and HQIC= 231.30. Furthermore, test statistics and corresponding value; Kolmogorov Smirnov (KS) = 0.065(p-value=0 .950), Anderson Darling (AD) = 0.215(p-value= 0.985), Cramer-von -Mises(W) = 0.037(p-value=0.949) with corresponding $p > 0.05$ suggest that data come from LPET. That is, model provides better fit for empirical data.

5.3.2. *Posterior predictive checks*

The observed mean time to failure (MTTF) is 7.126 hours and median time to failure (MTTF50) is 7.076. The MTTF and MTTF50 both are very close indicating that failure time distribution is approximately symmetric with no significant skewness in failure data.

This consistency supports this practical applicability of the model analyzing the conductor failure times.

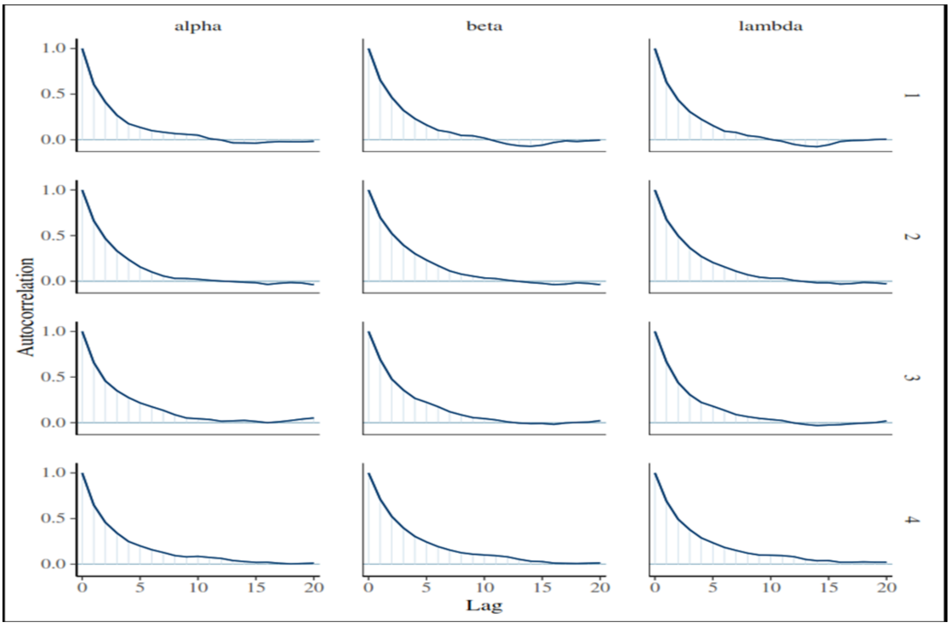

Fig. 8. Autocorrelations functions (ACFs) for all four parameters.

5.3.3. *Sensitivity analysis of the parameters*

Sensitivity analysis provides important insights into the influence of model parameters on reliability [49]. It helps to measure how strongly each parameter of the model affect a reliability metric (MTTF or MTTF50) using Normalized Local Sensitivity Index (NLSI). Let,$\theta \in \{\alpha, \beta, \lambda\}$.Also, let $g(\theta)$ is metric and θ_0 is estimated parameter either MLE or Posterior mean. Firstly, $g(\theta_0)$ was computed and then$g(\theta_+ = \theta + \Delta)$ and $g(\theta_- = \theta - \Delta)$. Again, we compute partial derivative that is approximated using symmetric finite difference by using $\frac{\partial g}{\partial \theta} = \frac{g(\theta_+) - g(\theta_-)}{2\Delta}$.

This provides the level of reliability measure changes due to slightly change in parameter. Finally, sensitivity index can be calculated using relation,

$$SI_\theta = \left| \frac{\theta_0}{g(\theta_0)} \cdot \frac{\partial g}{\partial \theta} \right|.$$

SI around zero indicates that parameter has little influence, Larger SI indicate that parameter has strong influence and SI with highest index indicates most influential parameter. In this study, we have applied MTTF () and sensitivity () function of R to measure SI.

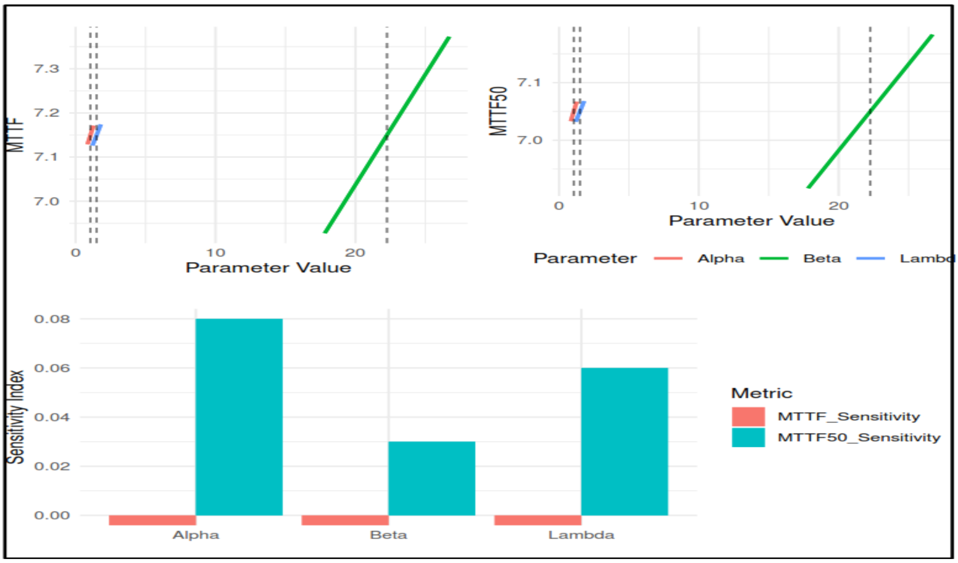

Fig. 9. Sensitivity analysis in LPET model.

The bar chart in Fig. 9 displays normalized sensitivity indices which is the proportion of the total variation that is attributed to all parameter individually after scaling by the sum of all effects. The bar height is not the raw magnitude of sensitivity. As shown in top plots, β has the steepest slope indicates β- parameter exhibits highest absolute change in MTTF as well as MTTF50 hence β is dominant driver of the LPET model. Normalization compresses the β index resulting not tall bar although it most influential parameter.

5.3.4. *Parameter correlations*

Table 13 shows pairwise correlation with strongest relationship of r = 0.943 between beta and lambda and of r = - 0.829 between alpha and beta. There is comparatively less correlation of r = -0.707 between alpha and lambda. These patterns of the correlations demonstrate appropriate parameter identifiability with no problematic multicollinearity.

Table 13. Pairwise parameter correlation.

	alpha	beta	lambda
alpha	1.000	-0.829	-0.707
beta	-0.829	1.000	0.943
lambda	-0.707	0.943	1.000

Fig. 10 shows the parameter correlations and marginal densities structurally consistent relationships within the LPET model.

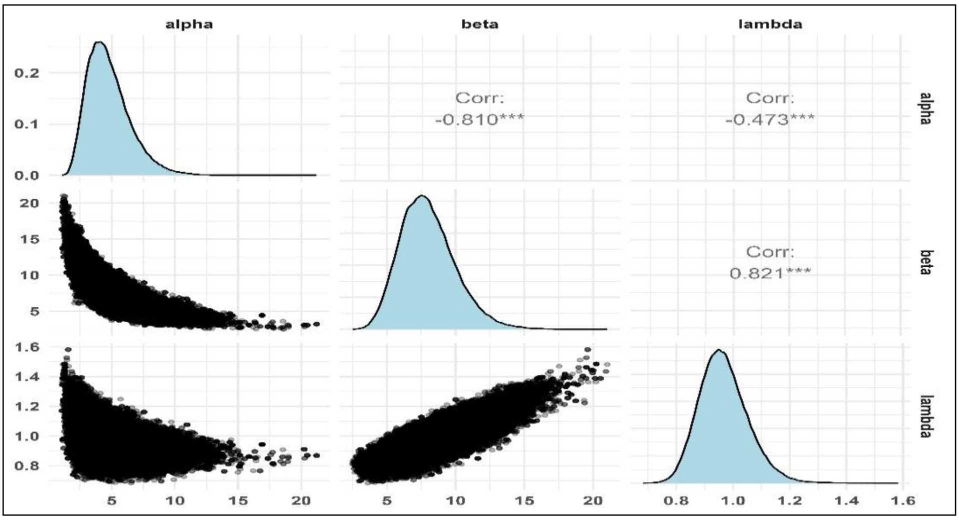

Fig. 10. Parameter correlations with densities.

Fig. 11 visualizes pairwise parameter dependencies using hexbin-density plots for different pairs of LPET parameters (α, β, λ) based on posterior sample obtained from Bayesian MCMC.

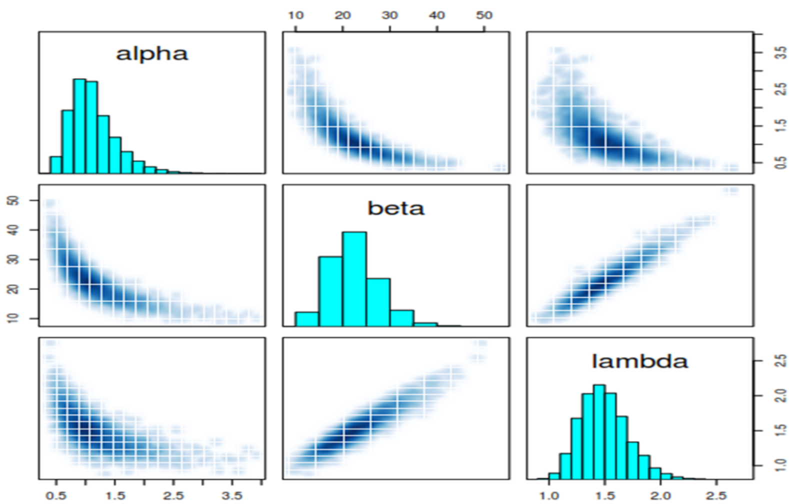

Fig. 11. Bayesian pairwise parameter relationships.

These plots are used when a pairwise scatterplot contain many points and cause overplotting. Darker region of this joint posterior density shows higher probability mass. That is, color intensity of the hexagons indicates the local density of MCMC sample. This allows visualization of parameter dependence, uncertainty and clustering. The off-diagonal scatterplots visually corroborate the correlation analysis. The parameters exhibit posterior dependence. The parameter α exhibits negative correlation with both β and λ while β, and λ show strong positive correlation. Marginal posteriors are unimodal confirming good MCMC mixing as well as well-defined posterior distribution.

Fig. 12 demonstrate posterior predictive distribution and predicted survival function. The observed data line represented by solid line runs smoothly through the middle of cloud (Simulated lines) indicated by blue line says that the LPET model accurately capturing the underlying failure process. plots demonstrate successful validation of model on reliability data set and provide strong confirmation of robustness and potentiality of the model.

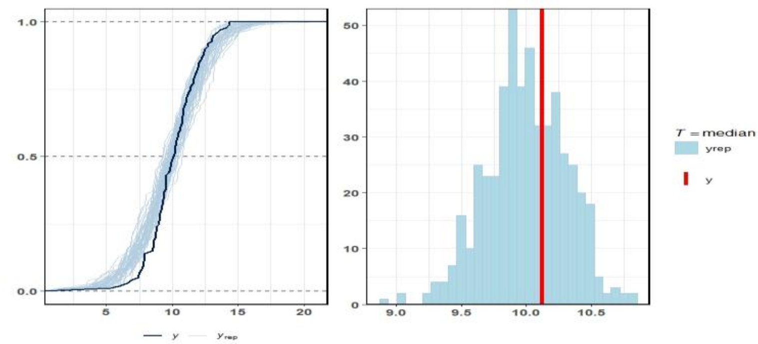

Fig. 12. Posterior predictive distribution shows close alignment with observed failure times.

Fig. 13 (left) displays the strong result of fitted LPET model versus the non-parametric Kaplan-Meier (KM) estimate. The LPET survival curve align very closely with the KM curve indicating excellent model fit of LPET to observed failure data. bar chart in right of Fig. 13 (right) displays minimal difference between predicted and empirical survival probabilities validating LPET model as accurate tool to analyze survival nature of the system for forecasting.

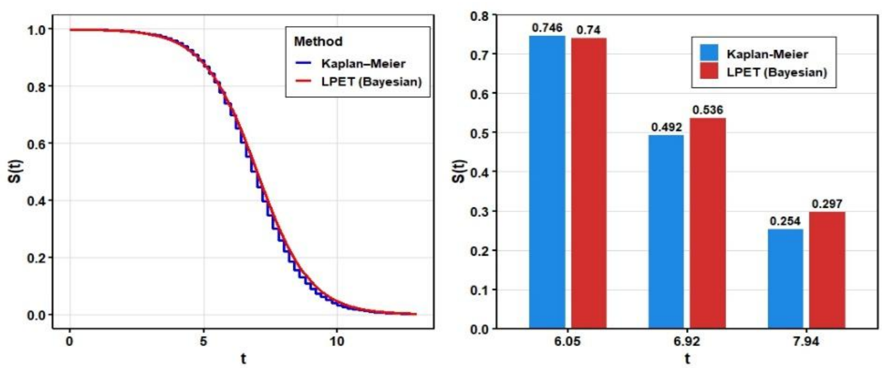

Fig. 13. KM vs LPET survival curves (Left) and bar chart (Right) for survival probabilities.

Fig. 14 validates the model's accuracy related to the failure dynamics. Figs. demonstrate the close alignment between Bayesian estimated hazard rate as well as the density function with their empirical plots verifying an excellent fitting of the model for given set of the data. That is, it is clear to say that model successfully replicates overall distribution of failure time density as well as the instantaneous risk of failures (Hazard).

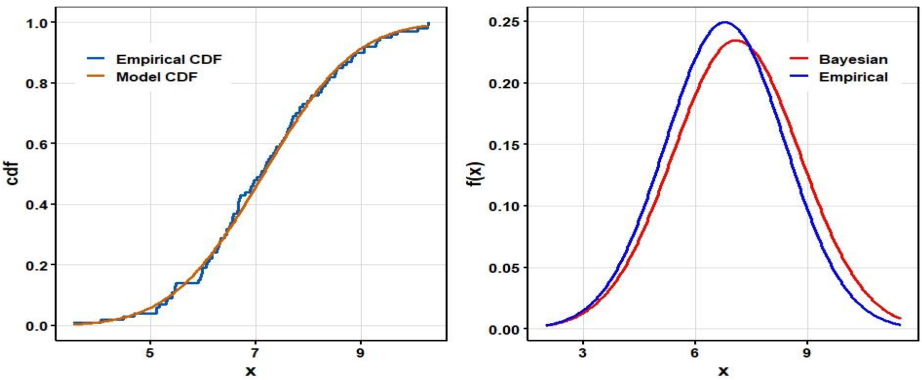

Fig. 14. Model Fit Assessment: Empirical vs. Model Hazard Function (Left) and Empirical vs. Model Density Function (Right).

5.3.5. *Survival characteristics*

Survival nature is displayed by present survival and reliability functions in Fig. 16. Here, MTTF is 7.15 and MTTF50 7.05 hours. The MTTF of 7.15 hours indicate that on average, failing of microcircuit occurs about 7 hours of operations Also, the bathtub shaped hazard rate confirms early random failures followed by wear-out.

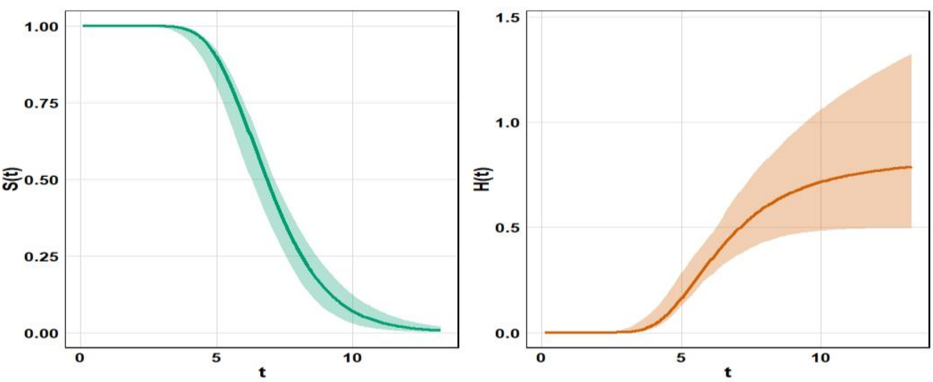

Fig. 15. Bayesian Posterior Estimates of the Survival and Hazard Rate Functions

The Bayesian posterior estimates displayed in Fig. 15 demonstrate that there is well characterized failure pattern. It also indicates that there are consistent reliability properties between approximately 7 to 7.15 hours. This evidence says that the LPET model can be effectively used for predicting component performances and planning maintenances schedules in industry and engineering fields.

5.4. *Model validation*

Comparison of the LL and AIC using the parameters estimated using Bayesian approach. For simplicity, only three classical models (Weibull, Log-normal and Exponential) are considered for comparison under Bayesian estimation. Lower values of AIC = 228.866 confirm that LPET model fits real data set precisely and will be competitive model in real data analysis (Table 14). Furthermore, the lowest WAIC and the DIC values also support the LPET model as superior model.

Table 14. Loglikelihood and AIC for LPET and other classical models using Bayesian estimation.

Model	LL	AIC	WAIC	ΔAIC	ΔWAIC	AIC Weight (%)	WAIC Weight (%)	DIC	pD
LPET	-111.43	228.86	227.50	0.00	0.00	17.3	72.3	250.30	13.71
Weibull	-112.50	228.99	230.40	0.13	2.90	25.5	17.0	260.11	17.554
Log-normal	-112.97	229.94	231.32	1.08	3.82	15.9	10.7	302.28	38.170
Exponential	-173.64	349.28	348.45	120.42	120.95	0.0	0.0	348.45	0.583

For comparisons of goodness-of-fit, KS, AD and CVM test statistics with corresponding p values are mentioned in Table 15. the resulting values with lower test statistics with higher p values support the LPET model as better among the competing models.

5.4.1. *Summary for goodness- of -Fit Tests*

The LPET model outperforms Weibull, Lognormal, and Exponential distributions in KS, AD and CVM test with all $p > 0.05$ stating no evidence against LPET.

Table 15. Goodness-of-fit.

Model	KS	p-value	AD	p-value	CVM	p-value
LPET	0.0661	0.9446	0.2167	0.9852	0.0375	0.9470
Weibull	0.0958	0.06159	0.4786	0.7680	0.0845	0.6683
Log-normal	0.0867	0.7335	0.3731	0.8744	0.0605	0.8131
Exponential	0.4302	0.0000	16.3441	0.0000	3.4306	0.0000

Fig. 16 (left) demonstrate the histogram plots of data and fitted density plots of LPET (MLE and Bayesian) and competing models Weibull, Lognormal and Exponential. Similarly Fig. 16 (right) demonstrate ECDF against the fitted pdf of LPET as well as competing models. ECDF and Histogram comparisons confirm LPET's superior fit over competitors.

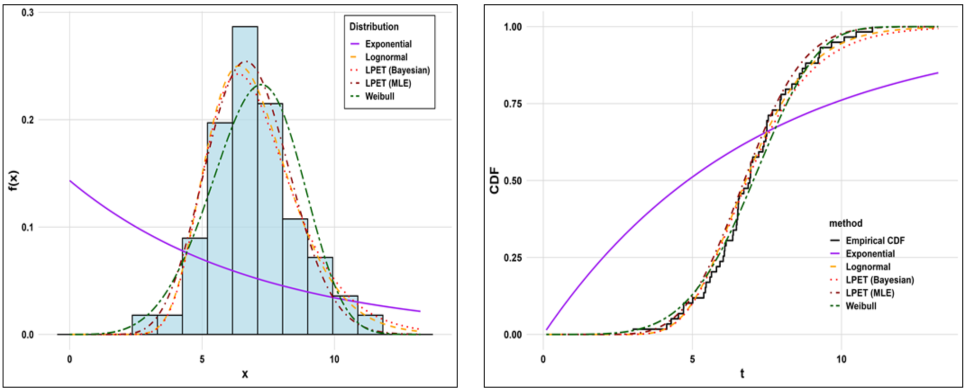

Fig. 16. Histogram vs fitted LPET (left) and ECDF vs Fitted CDF (right), Weibull, Lognormal and Exponential.

Fig. 17 demonstrates the KM plots for LPET model versus the competing models taken in cosideratons.

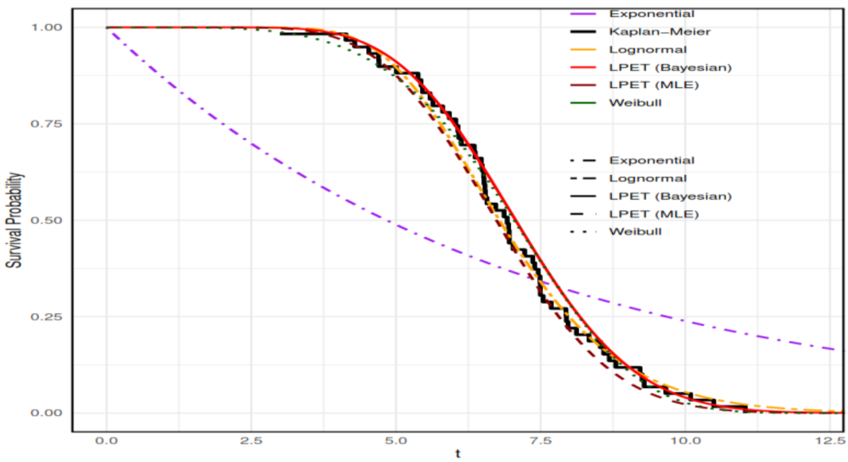

Fig. 17. Kaplan- Meier curve vs LPET survival vs Weibull, Lognormal and exponential.

5.5. *Competitive performance analysis*

The LPET model demonstrated excellent competitive performance, ranking first among the six-distribution tested. LPET model outperformed 5 out of 6 competing distribution (83 % of competitors). Around 7.22 % AIC over Generalized Gamma (3 parameters), 4.69 % over Log-Logistic (2 Parameters) and outperformed Weibull and Log-Normal distributions. Also, LPET model demonstrated 34.47 % improvement over Exponential distribution.

5.6. *Goodness-of-Fit test results for LPET distribution*

Goodness-of-fit Test for LPET Distribution were found as; Kolmogorov- Smirnov test statistics 0.066(p-value 0.946), Anderson-Darling statistic 0.985(p-value 0.985) and Cramer-von-Mises statistic 0.037(p-value 0.949). All the goodness-of-fit test yielded p values > 0.05 indicating that there is no evidence against the hypothesis that data follows LPET model (Table 16). The use of parametric bootstrap for Kolmogorov-Smirnov p-values follows recommendations from current inference based on lifetime distributions [50]. Also, employing parametric bootstrap procedure to obtain *p*-values for Kolmogorov -Smirnove test, we assessed the adequacy of the models.

Table 16. Kolmogorov- Smirnov test with Parametric Bootstrap.

Distribution	KS-statistics	Bootstrap p- value	Adequate Fit
LPET	0.0657	0.074	Yes
Gamma	0.0710	0.672	Yes
Weibull	0.0958	0.152	Yes
Log-Normal	0.0867	0.324	Yes
Exponential	0.4302	0.0001	No

Among all flexible models, LPET demonstrate the best fit.

5.7. *Survival characteristics and reliability metrics*

Bayesian analysis demonstrated following key reliability metrics

Mean survival Time (MST): 7.15 hours (955 CI: 6.92-7.38); Median survival Time (MST50): 7.08 hours (95 % CI: 6.85-7.31). The close agreement between MST and MST50 indicate approximately symmetric failure time distribution.

6. Discussion

This study has introduced the LPET distribution, a novel three-parameter lifetime model. The model is developed through Lehmann-type exponentiation of an exponential Extension baseline with power transformation of variable x. The LPET model provides a theoretically flexible framework for reliability data which combine exponentiation and power transformation to enable multiphase hazard rate shapes which are generally unattainable by existing exponential families.

6.1. *Theoretical contribution and model flexibility*

Dual-parameterization strategy is the principal innovation of the LPET model. The exponentiation parameter α behaves as a frailty parameter which captures unobserved heterogeneity. The other parameter λ controls the tail behavior and failure accumulation rate. Combinations of these change permits the model to adapt to both early-life and wear-out failure phases.

6.2. *Estimation performance and consistency*

The simulation study confirms that LPET are statistically consistent and efficient. As small sample size increased from n =100 to n =1000, bias, MSE, and RMSE decreased markedly across all three parameter sets (Tables 1-3). Convergence rates exceeded 0.9 for all but smallest samples which confirm numerical stability. Notably, LPET shows lower bias and MSE compared to Weibull, Lognormal, and Exponential models under equivalent settings (Table 4).

6.3. *Empirical validation and comparative advantages*

Application to the microcircuit electromigration failure dataset reaffirmed the LPET model's practical utility. With lowest AIC (228.86) and highest p- values in Kolmogorov-Smirnov (0.946), Anderson-Darling (0.985) and Cramer-von Mises (0.949) tests, LPET outperformed all eleven competing models (Table 7). The Kaplan-Meier survival very closely coincides with narrower creditable intervals. The estimated MTTF =7.13 hours providing a practical and specific benchmark.

6.4. *Bayesian robustness and sensitivity*

The Bayesian analysis further validated the model's robustness. Posterior estimates closely matched MLEs (Table 9). The MCMC diagnostics indicates excellent convergence (R-hat = 1.00 and ESS > 2000). Furthermore, the sensitivity analysis showed that beta is most influencing parameter. alternative priors (Gamma and Lognormal) showed minimal variation in posterior summaries (Table 11) which confirms that inferences are not unduly influenced by prior specification. The model's generalizability was supported by predictive accuracy measures (LOOIC= 227.56, WAIC= 227.50).

6.5. *Limitations of study*

Further studies for large and different data sets may influence the results as well as computations for Bayesian inference may be intensive under 4 chains each with 50000 iterations. This study analyzed uncensored data so the performances under right or interval censoring may remain unexplored.

6.6. *Future work of the study*

Applications of LPET model to censored survival data, truncated data and multivariate regression settings may be the future work. Furthermore, exploration of accelerated life test extension may be the subject of further study.

7. Conclusions

This study provides a significant theoretical contribution to survival analysis and reliability engineering introducing of a novel LPET distribution. The model is formulated through a Lehmann-type exponentiation of Exponential Extension family, incorporating a frailty parameter (α) and reparametrized power λ. The LPET model grant the extra flexibility, enabling it to capture a wide range of hazard shapes data such as bathtub, J-shaped and inverted *J*-shaped and will be very useful in modern engineering system. Practical applicability and robustness of model were rigorously validated by extensive analysis. Simulation studies demonstrated the consistency and accuracy of the estimation. Applicability using a real- world microcircuit failure dataset and significantly outperformed eleven competitive probability models. The Lowest Akaike information Criteria (AIC=228.87) and excellent result of Kolmogorov -Smirnov goodness of fit test (KS=0.066, p-value=0.946) verified the excellency of the model. Also, the Excellent MCMC convergence (R-hat =1.00) supported model and mean time to failure (MTTF) of 7.126 hours as well as median time to failure (MTTF50) of 7.075 hours proved model's practical precision. Future work of the study will focus on extension of applicability of LPET model on various field of datasets of medical, and engineering. These extension of the model in other field would solidify the LPET distribution as a powerful and versatile probability model in reliability analysis.

Acknowledgment

The author wishes to express gratitude to colleagues, seniors and family members for their encouragement, discussions, and guidance throughout this research.

References

1. Y. M. Du and C. P. Sun, Reliab. Eng. Syst. Saf. **228**, ID 108756 (2022). https://doi.org/10.1016/j.ress.2022.108756
2. D. R. Cox and N. Reid, J. R. Stat. Soc. Ser. B **49**, 1 (1987). https://doi.org/10.1111/j.2517-6161.1987.tb01422.x
3. G. S. Mudholkar and D. K. Srivastava, IEEE Trans. Reliab. **42**, 299 (1993). https://doi.org/10.1109/24.229504
4. G. M. Cordeiro and M. De Castro, J. Stat. Comput. Simul. **81**, 883 (2011).
5. R. D. Gupta and D. Kundu, Aust. N. Z. J. Stat. **41**, 173 (1999). https://doi.org/10.1111/1467-842X.00072
6. M. Irshad, S. Aswathy, R. Maya, A. I. Al-Omari, and G. Alomani, AIMS Math. **9**, 24810 (2024).
7. A. Jamal, I. Alhribat, and M. H. Samuh, J. Stat. Res. **58**, 279 (2025). https://doi.org/10.3329/jsr.v58i2.80609
8. L. B. S. Telee and V. Kumar, Pravaha **28**, 11 (2022). https://doi.org/10.3126/pravaha.v28i1.57966
9. P. Cheng, L. F. Mao, W. H. Shen, and Y. L. Yan, Electronics **14**, 3151 (2025). https://doi.org/10.3390/electronics14153151

10. N. Eugene, C. Lee, and F. Famoye, Commun. Stat.-Theory Methods **31**, 497 (2002). https://doi.org/10.1081/STA-120003130
11. P. E. Oguntunde, O. S. Babatunde, and A. O. Ogunmola, Int. J. Stat. Appl. **4**, 113 (2014).
12. L. B. S. Telee and V. Kumar, Int. J. Eng. Sci. Technol. **7**, 17 (2023). https://doi.org/10.29121/ijoest.v7.i5.2023.535
13. M. J. S. Khan and B. Khatoon, Pak. J. Stat. Oper. Res. **15**, 547 (2019). https://doi.org/10.18187/pjsor.v15i3.2716
14. G. M. Cordeiro, E. M. Ortega, and G. O. Silva, J. Stat. Comput. Simul. **81**, 827 (2011). https://doi.org/10.1080/00949650903517874
15. A. H. Muse, A. Almohaimeed, H. N. Alqifari, and C. Chesneau, PLoS One **20**, ID e0307410 (2025). https://doi.org/10.1371/journal.pone.0307410
16. J. K. Kruschke, J. Exp. Psychol. Gen. **142**, 573 (2013). https://doi.org/10.1037/a0029146
17. M. Orlitzky, Organ. Res. Methods **15**, 199 (2012). https://doi.org/10.1177/1094428111428356
18. M. J. Zyphur and F. L. Oswald, J. Manage. **41**, 390 (2015). https://doi.org/10.1177/0149206313501200
19. X. Jia, W. Hou, and C. Papadimitriou, J. Reliab. Sci. Eng. **1**, ID 025002 (2025). https://doi.org/10.1088/3050-2454/adc580
20. L. Leoni, F. BahooToroody, S. Khalaj, F. D. Carlo, A. BahooToroody, and M. M. Abaei, Int. J. Environ. Res. Public Health **18**, 3349 (2021). https://doi.org/10.3390/ijerph18073349
21. B. Abba, M. Muhammad, M. S. Isa, and J. Wu, Methodology (2025). https://doi.org/10.48550/arXiv.2502.11507
22. W. S. Zhao, R. Zhang, and D. W. Wang, Micromachines **13**, 883 (2022). https://doi.org/10.3390/mi13060883
23. H. H. Ahmad, O. E. Abo-Kasem, A. Rabaiah, and A. Elshahhat, AIMS Math. **10**, 10228 (2025). https://doi.org/10.3934/math.2025466
24. F. Jaderi, Z. Z. Ibrahim, and M. R. Zahiri, Process Saf. Environ. Prot. **121**, 312 (2019). https://doi.org/10.1016/j.psep.2018.11.005
25. Z. Y. Han and W. G. Weng, J. Hazard. Mater. **189**, 509 (2011). https://doi.org/10.1088/3050-2454/adc580
26. T. Abbasi, V. Kumar, S. Tauseef, and S. Abbasi, J. Chem. Health Saf. **25**, 19 (2018). https://doi.org/10.1016/j.jchas.2018.02.004
27. R. K. Joshi and V. Kumar, Int. J. Math. Stat. Invent. **8**, 35 (2020).
28. Z. A. Al-saiary, R. A. Bakoban, and A. A. Al-zahrani, Mathematics **8**, 23 (2019). https://doi.org/10.3390/math8010023
29. J. Moors, The Statistician **37**, 25 (1988). https://doi.org/10.2307/2348376
30. H. Boureji and A. Sayah, J. Stat. Res. **59**, 183 (2026). https://doi.org/10.3329/jsr.v59i2.88064
31. H. A. Schafft, T. C. Station, J. Mandel, and J. D. Shott, IEEE Trans. Electron Devices **ED-34**, 673 (1987). https://doi.org/10.1109/T-ED.1987.22979
32. W. Nelson and N. Doganaksoy, in Recent Advances in Life-Testing and Reliability, ed. N. Balakrishnan (CRC Press, Boca Raton, 1995) pp. 377–408. https://doi.org/10.1201/9781003418313-21
33. R Core Team, R: A Language and Environment for Statistical Computing (R Foundation for Statistical Computing, Vienna, 2024).
34. A. K. Chaudhary and L. B. Sah Telee, J. Nepal Math. Soc. **7**, 1 (2024). https://doi.org/10.3126/jnms.v7i1.67483
35. Y. Tang, M. Xie, and T. N. Goh, Commun. Stat.-Theory Meth. **32**, 913 (2003). https://doi.org/10.1081/STA-120019952
36. I. Ghosh and G. G. Hamedani, Int. J. Stat. Probab. **4**, 94 (2015). https://doi.org/10.5539/ijsp.v4n3p94
37. D. Bhati, M. A. Malik, and H. J. Vaman, Metron **73**, 335 (2015). https://doi.org/10.1007/s40300-015-0060-9
38. R. M. Smith and L. J. Bain, Commun. Stat.-Theory Meth. **4**, 469 (1975). https://doi.org/10.1080/03610927508827263

39. C. D. Lai, M. Xie, and D. N. P. Murthy, IEEE Trans. Reliab. **52**, 33 (2003). https://doi.org/10.1109/TR.2002.805788
40. S. Nadarajah and S. Kotz, Reliab. Eng. Syst. Saf. **91**, 689 (2006). https://doi.org/10.1016/j.ress.2005.05.008
41. A. Gelman and C. R. Shalizi, Br. J. Math. Stat. Psychol. **66**, 8 (2013). https://doi.org/10.1111/j.2044-8317.2011.02037.x
42. M. Ibrahim, C. Adams, and A. El-Zaart, JISTEM-J. Inf. Syst. Technol. Manag. **12**, 559 (2015). https://doi.org/10.4301/S1807-17752015000300004
43. D. Kundu and K. Das, J. Stat. Res. **58**, 111 (2024). https://doi.org/10.3329/jsr.v58i1.75417
44. H. A. Rasheed and M. N. Abd, Ibn AL-Haitham J. Pure Appl. Sci. **36**, 289 (2023). https://doi.org/10.30526/36.2.2946
45. J. H. Tay, A. Kocher, and S. Duchene, PLOS Comput. Biol. **20**, ID e1012371 (2024). https://doi.org/10.1371/journal.pcbi.1012371
46. A. Vehtari, A. Gelman, and J. Gabry, Stat. Comput. **27**, 1413 (2017). https://doi.org/10.1007/s11222-016-9696-4
47. S. Watanabe and M. Opper, J. Mach. Learn. Res. **11**, 3571 (2010).
48. A. Gelman and D. B. Rubin, Stat. Sci. **7**, 457 (1992). https://doi.org/10.1214/ss/1177011136
49. D. Kong, S. Lu, L. Feng, and Q. Xie, J. Fire Sci. **29**, 317 (2011). https://doi.org/10.1177/0734904110396314
50. W. Panichkitkosolkul, K. Khruachalee, and A. Volodin, J. Stat. Res. **59**, 107 (2025). https://doi.org/10.3329/jsr.v59i1.83689